

Novel single or double insertion of alkynes into rhodium– and iridium–oxygen or –phosphorus atom bonds and transannular addition of 1-alkynes between the rhodium atom and the *ipso*-carbon atom of the phosphorus ligand

Yasuhiro Yamamoto,* Kenichiro Sugawara and Xiao-Hong Han

Department of Chemistry, Faculty of Science, Toho University, Miyama, Funabashi, Chiba 274-8510, Japan. E-mail: yamamoto@chem.sci.toho-u.ac.jp

Received 1st June 2001, Accepted 1st November 2001

First published as an Advance Article on the web 20th December 2001

Reactions of Cp^{*}MCl(MDMPP-*P,O*) (**1a**: M = Rh; **1b**: M = Ir; MDMPP-*P,O* = PPh₂(C₆H₃-2-MeO-6-*O*)) or Cp^{*}MCl(BDMPP-*P,O*) (**2a**: M = Rh; **2b**: M = Ir; BDMPP-*P,O* = PPh(C₆H₃-2,6-(MeO)₂)(C₆H₃-2-(MeO)-6-*O*)) with 1-alkynes were carried out in the presence of KPF₆. Complex **1a** reacted with HC≡CR (R = Ph, *p*-tolyl) to give [Cp^{*}Rh{PPh₂(C₆H₃-2-(MeO)-6-(*O*-CR=CHCH=CR))}] (PF₆) **5** bearing the (*P,O,C*) tridentate ligand derived from a head-to-head dimerization of 1-alkynes, whereas reaction with *n*BuC≡CH gave a head-to-tail double insertion complex **6**, however the reactions of **1b** in MeOH gave carbene complexes [Cp^{*}Ir{PPh₂(C₆H₃-2-(MeO)-6-*O*)-(=C(OMe)CH₂R)}] (PF₆) **13** and a carbonyl complex [Cp^{*}Ir(CO){PPh₂(C₆H₃-2-(MeO)-6-*O*)}] (PF₆) **14**. Rhodium complexes **1a** and **2a** afforded [Cp^{*}Rh(CO){PPh₂(C₆H₃-2-(MeO)-6-(*O*CH=C(COOR))}] (PF₆) **8** or [Cp^{*}Rh(CO){PPh(C₆H₃-2,6-(MeO)₂)(C₆H₃-2-(MeO)-6-(*O*CH=C(COOR))}] (PF₆) **11** on treatment with HC≡CCOOR (R = Me, Et). Reactions of **1a**, **1b**, **2a** or **2b** with ROOC≡CCOOR (R = Me, Et) gave [Cp^{*}MCl{PPh₂(C₆H₃-2-(MeO)-6-(*O*C(COOR)=C(COOR))}] (**9**: M = Rh, **17**: M = Ir) and [Cp^{*}MCl{PPh(C₆H₃-2,6-(MeO)₂)(C₆H₃-2-(MeO)-6-(*O*C(COOR)=C(COOR))}] (**12**: M = Rh, **18**: M = Ir), respectively. Reactions of **1a** or **1b** with HC≡CC₆H₄-4-COOMe bearing an electron-withdrawing substituent gave the head-to-head double insertion products (**5c**: M = Rh; **16**: M = Ir) and Cp^{*}MCl₂[PPh₂{CH=C(C₆H₃-4-COOMe)(C₆H₃-2-(MeO)-6-(*O*H))}] (**7**: R = Rh; **15**: R = Ir), and resulted in a *cis*-insertion into the P–C bond of the phosphine ligand and a cleavage of the Rh–O bond. Reaction with **2a** afforded **10a**, derived from a transannular addition of 1-alkyne between the Rh atom and the *ipso*-carbon atom of the phosphine ligand. Reactions of **9** with CO or isocyanides (L) in the presence of KPF₆ or Ag(CF₃SO₃) gave [Cp^{*}Rh(L){PPh₂(C₆H₃-2-(MeO)-6-(*O*C(COOR)=C(COOR))}]X (L = XylNC, MesNC, CO; X = PF₆, CF₃SO₃). Structural data for some complexes obtained here are described. The reaction mechanism is discussed.

Introduction

Metal alkynyl complexes are currently of great interest^{1,2} since they can be used as valuable synthons for constructing vinylidene or carbene complexes for use in organic synthesis.^{3–8} Reactions of organotransition metal halides with 1-alkynes in the presence of anions such as PF₆[−], BF₄[−], and CF₃SO₃[−], are representative among the preparative methods of vinylidene complexes.⁹ One *ortho*-methoxy group in (2,6-dimethoxyphenyl)diphenylphosphine can be demethylated in the reaction with iso-electronic complexes [Cp^{*}MCl₂]₂ (M = Rh or Ir; Cp^{*} = pentamethylcyclopentadienyl) or [(η⁶-arene)RuCl₂]₂ (η⁶-arene = C₆Me₆, *p*-cymene, C₆H₃Me₃), giving corresponding metal complexes with a (*P,O*) chelating phosphine, (η⁶-arene)RuCl(MDMPP-*P,O*)^{10,11} or Cp^{*}MCl(MDMPP-*P,O*)^{12,13} (Cp^{*} = C₅Me₅; MDMPP-*P,O* = PPh₂(C₆H₃-2-(MeO)-6-*O*)). We have recently reported the unprecedented insertion of tcne (or tenq) into the C–H bond adjacent to the M–O bonds, producing Cp^{*}MCl[PPh₂{C₆H₂-2-(MeO)-5-(C(CN)₂C(CN)₂H)-6-*O*}] when the aforementioned rhodium(III) and iridium(III) complexes were treated with tcne or tenq.¹⁴

We have also reported that treatment of the ruthenium(II) complex with PhC≡CH in the presence of NaPF₆ in a mixture of acetone and CH₂Cl₂, afforded a vinylidene complex, [(η⁶-C₆Me₆)Ru(MDMPP-*P,O*)(=C=CHPh)](PF₆).¹⁵ This reaction is one of the well known preparative methods for vinylidene complexes.⁹ However, the treatment of Cp^{*}RhCl(MDMPP-*P,O*) **1a** with 1-alkynes such as HC≡CCOOMe, PhC≡CH and

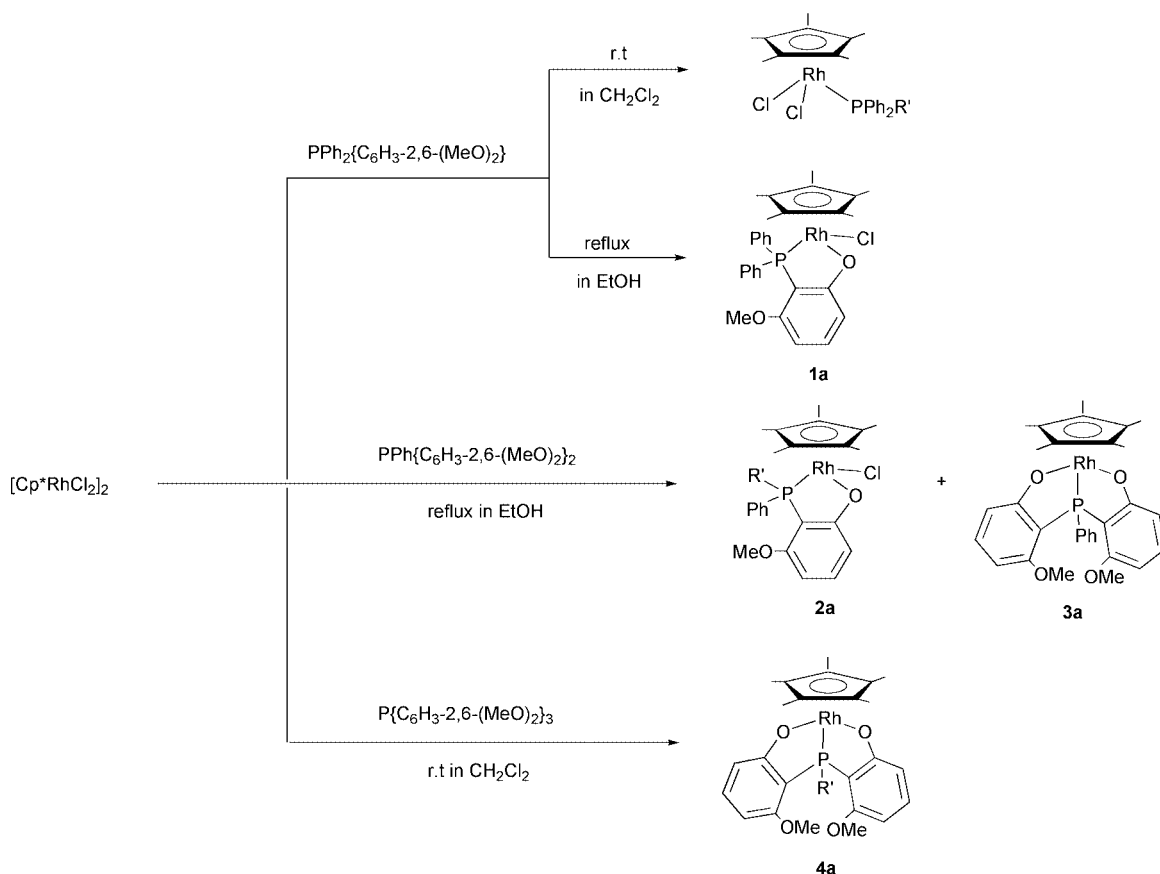
*n*BuC≡CH, and disubstituted alkynes such as C₂(CO₂R)₂ (R = Me, Et) in the presence of NaPF₆ or KPF₆ led to unusual reactions; in the reaction with HC≡CCOOMe, an extraction of CO from an ester group and the insertion of another 1-alkyne into an Rh–O σ-bond occurred, producing a seven-membered metallocycle, and reactions with HC≡CR (R = Ph, *n*Bu) led to the formation of complexes bearing five- and six-membered rings accompanying a double insertion of 1-alkynes into an Rh–O σ-bond. Treatment with disubstituted alkynes also led to a single insertion into a Rh–O σ-bond. A similar insertion of unsaturated molecules into the metal–oxygen bond of platinum alkoxides has been achieved with perfluoro-olefins¹⁶ such as CF₂=CF₂ and hexafluorocyclobutene. In this study, the insertion of alkyne into the transition metal–O σ-bonds is performed for the first time.^{17,18} These unprecedented reactions allow control of single and double insertion of alkynes into the metal–O bond of pentamethylcyclopentadienyl-rhodium and –iridium complexes bearing the (*P,O*) bidentate ligands by variation of the alkyne substituents.

Part of this work has already been published.^{19,20}

Results and discussion

Reactions of [Cp^{*}RhCl₂]₂ with (2,6-dimethoxyphenyl)diphenylphosphine or bis(2,6-dimethoxyphenyl)phenylphosphine

We previously reported that the reaction of [Cp^{*}RhCl₂]₂ with PPh₂(C₆H₃-2,6-(MeO)₂) at room temperature gave Cp^{*}RhCl₂-



Scheme 1 Reactions of $[\text{Cp}^*\text{RhCl}_2]_2$ with (2,6-dimethoxyphenyl)diphenylphosphine, bis(2,6-dimethoxyphenyl)phenylphosphine or tris(2,6-dimethoxyphenyl)phosphine ($\text{R}' = 2,6\text{-(MeO)}_2\text{C}_6\text{H}_3$).

$\{\text{PPh}_2(\text{C}_6\text{H}_3\text{-}2,6\text{-(MeO)}_2)\}$ in high yield, whereas the reaction at reflux in EtOH resulted in demethylation of the phosphine forming $\text{Cp}^*\text{RhCl}(\text{MDMPP-}P,O)$ **1a**, showing a bidentate P,O coordination.¹² In this study, a mixture of $[\text{Cp}^*\text{RhCl}_2]_2$ and bulky bis(2,6-dimethoxyphenyl)phenylphosphine was heated in EtOH, causing the demethylation of one or two methyl groups of the phosphine and giving two orange complexes, $[\text{Cp}^*\text{RhCl}(\text{BDMPP-}P,O)]$ **2a** ($\text{BDMPP-}P,O = \text{PPh}\{\text{C}_6\text{H}_3\text{-}2,6\text{-(MeO)}_2\}\{\text{C}_6\text{H}_3\text{-}2\text{-(MeO)-}6\text{-}O\}$) and $[\text{Cp}^*\text{Rh}\{\text{PPh}(\text{C}_6\text{H}_3\text{-}2\text{-(MeO)-}6\text{-}O)_2\}]$ **3a** as separated by chromatography on deactivated alumina (containing 10% H_2O) (Scheme 1).

It was confirmed by X-ray analysis that **2a** consists of a $\text{Rh}_R\text{P}_R/\text{Rh}_S\text{P}_S$ pair (Fig. 1). Diastereomers could in principle exist in **2a** which has two chiral centers, however the ^1H NMR spectra revealed that **2a** consists of only the one diastereomer at room temperature and at -60°C , exhibiting one doublet at δ 1.34 due to pentamethylcyclopentadienyl protons. The methoxy protons appeared at δ 3.08, 3.25 and 3.74 as sharp singlets. The inequivalence for the methoxy protons is assumed to arise from either the presence of a chiral center of the P atom or restricted rotation of the $\text{C}_6\text{H}_3(\text{OMe})_2$ ring about the P-C axis.

It has been reported that the complexes $(\eta^6\text{-arene})\text{RuCl}(\text{BDMPP-}P,O)$ ($\eta^6\text{-arene} = 1,2,3,4\text{-Me}_4\text{C}_6\text{H}_2$ *p*-cymene, 1,3,5- $\text{Me}_3\text{C}_6\text{H}_3$) derived from the reactions of $[(\eta^6\text{-arene})\text{RuCl}_2]_2$ with $\text{PPh}\{\text{C}_6\text{H}_3\text{-}2,6\text{-(MeO)}_2\}_2$ exist as two diastereomers in solutions and as a $\text{Ru}_R\text{P}_R/\text{Ru}_S\text{P}_S$ pair in the solid state.^{10,11} It was found that reaction with bulky tris(2,6-dimethoxyphenyl)phosphine, $\text{P}\{\text{C}_6\text{H}_3\text{-}2,6\text{-(MeO)}_2\}_3$, readily induced demethylation of the two methyl groups even at room temperature, affording $\text{Cp}^*\text{Rh}\{P(\text{C}_6\text{H}_3\text{-}2,6\text{-(MeO)}_2)(\text{C}_6\text{H}_3\text{-}2\text{-(MeO)-}6\text{-}O)_2\}$ **4a** containing a P,O,O' -tridentate ligand. The ^1H NMR spectrum indicated two singlets at δ 3.42 and 3.49 due to methoxy protons. The detailed structure of **4a** was confirmed by X-ray analysis (Fig. 2). The degree of demethylation decreased with decrease of bulkiness of the phosphine ligand.

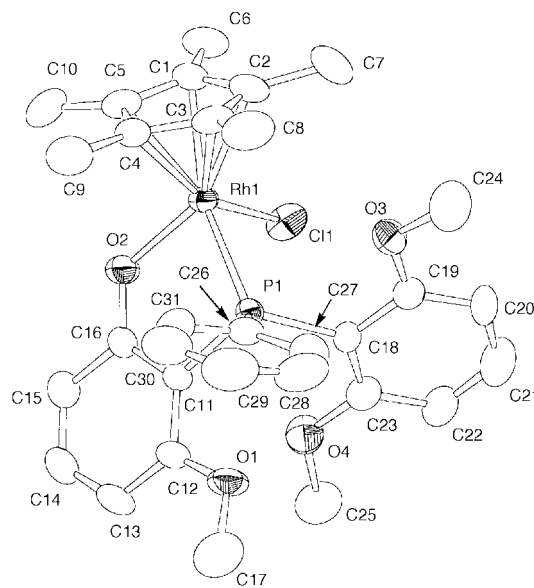


Fig. 1 Molecular structure of **2a**; thermal ellipsoids are drawn to encompass 50% probability.

Similar reactive behavior has been noted in the reactions of $[(\eta^6\text{-arene})\text{RuCl}_2]_2$ with these phosphines.^{10,11}

Reactions of $[\text{Cp}^*\text{RhCl}(\text{MDMPP-}P,O)]$ **1a** with alkynes

Reaction of **1a** with an excess of ethynylbenzene or ethynyltoluene in the presence of KPF_6 or NaPF_6 at room temperature gave orange complexes $[\text{Cp}^*\text{Rh}\{\text{PPh}_2(\text{C}_6\text{H}_3\text{-}2\text{-(MeO)-}6\text{-}O\text{-}(\text{OCR}=\text{CHCH}=\text{CR}))\}](\text{PF}_6)$ (**5a**: $\text{R} = \text{Ph}$; **5b**: $\text{R} = 4\text{-tolyl}$) (Scheme 2). X-Ray analyses of **5a**¹⁹ and **5b** revealed that a Rh atom is surrounded by a novel (P, O, C) tridentate ligand resulting from a head-to-head double-insertion of 1-alkyne into the Rh-O

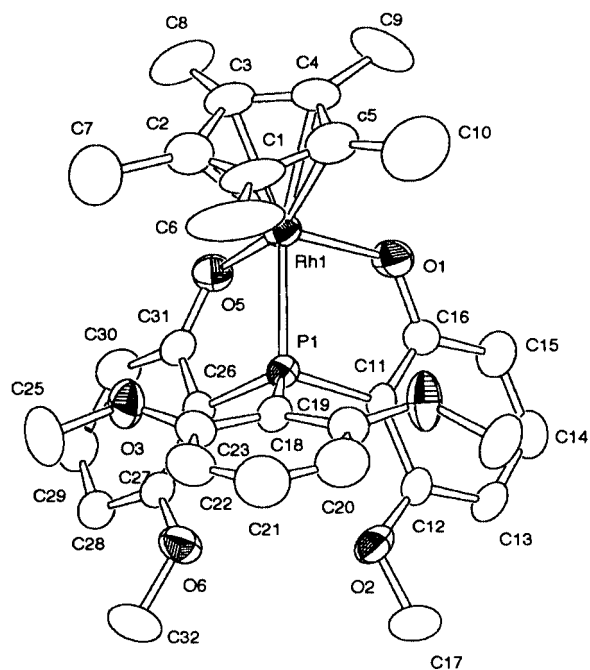


Fig. 2 Molecular structure of **4a**; thermal ellipsoids are drawn to encompass 50% probability.

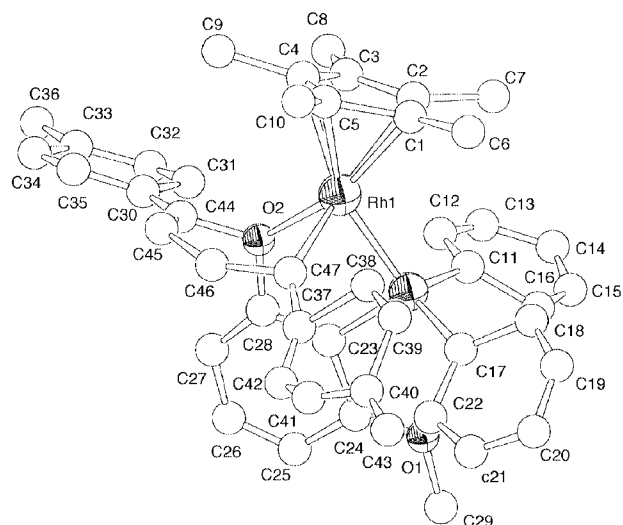


Fig. 3 Molecular structure for the complex cation of **5b**; the PF_6 cation was omitted for clarity and thermal ellipsoids are drawn to encompass 50% probability.

bond (Fig. 3). Two carbon atoms bearing a phenyl group are connected to the rhodium and oxygen atoms. The molecule contains five- and six-membered rings through coordination of an ether-O atom. A similar double insertion proceeded on treatment of **1a** with 1-hexyne, giving $[\text{Cp}^*\text{Rh}\{\text{PPh}_2(\text{C}_6\text{H}_3-2-(\text{MeO})-6-(\text{OC}(n\text{Bu})=\text{CHC}(n\text{Bu})=\text{CH}))\}]\text{PF}_6$ **6**; X-ray analysis revealed that the structure consists of a head-to-tail double insertion and a *n*-butyl-substituted carbon atom connected to the O atom (Fig. 4). An olefinic proton in the Rh–CH= moiety appeared at δ 5.69 as a doublet due to coupling with ^{103}Rh . A similar insertion of two $\text{PhC}\equiv\text{CH}$ molecules into an Ru–N bond has recently been reported to occur on the triruthenium cluster $[\text{Ru}_3(\mu\text{-H})(\mu\text{-N}=\text{CPh}_2)(\text{CO})_{10}]$.²¹ An attempt to release the ether O-coordination with xyllyl isocyanide was carried out at room temperature for **5a**, however the starting compounds were recovered quantitatively, demonstrating the strength of the ether coordination and the higher stability of five- and six-membered rings.

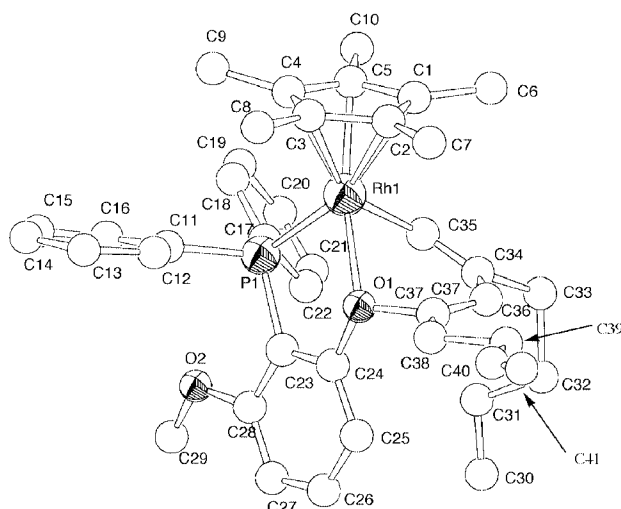


Fig. 4 Molecular structure for the complex cation of **6**; the PF_6 cation was omitted for clarity and thermal ellipsoids are drawn to encompass 50% probability.

Complex **1a** in a mixture of acetone and CH_2Cl_2 reacted with $\text{HC}\equiv\text{CC}_6\text{H}_4\text{COOMe-4}$ bearing an electron-withdrawing substituent at 4-position of the phenyl group in the presence of KPF_6 to give the head-to-head double insertion complex **5c**, $[\text{Cp}^*\text{Rh}\{\text{PPh}_2(\text{C}_6\text{H}_3-2-(\text{MeO})-6-(\text{OC}(\text{C}_6\text{H}_4-4\text{-COOMe})=\text{CHCH}=\text{C}(\text{C}_6\text{H}_4-4\text{-COOMe}))\}]\text{PF}_6$ (Fig. 5) and $\text{Cp}^*\text{RhCl}_2\text{-}[\text{PPh}_2\{\text{CH}=\text{C}(\text{C}_6\text{H}_4-4\text{-COOMe})(\text{C}_6\text{H}_3-2-(\text{MeO})-6-(\text{OH}))\}]\text{7}$.

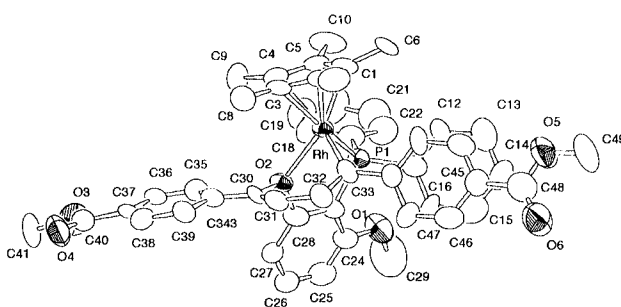
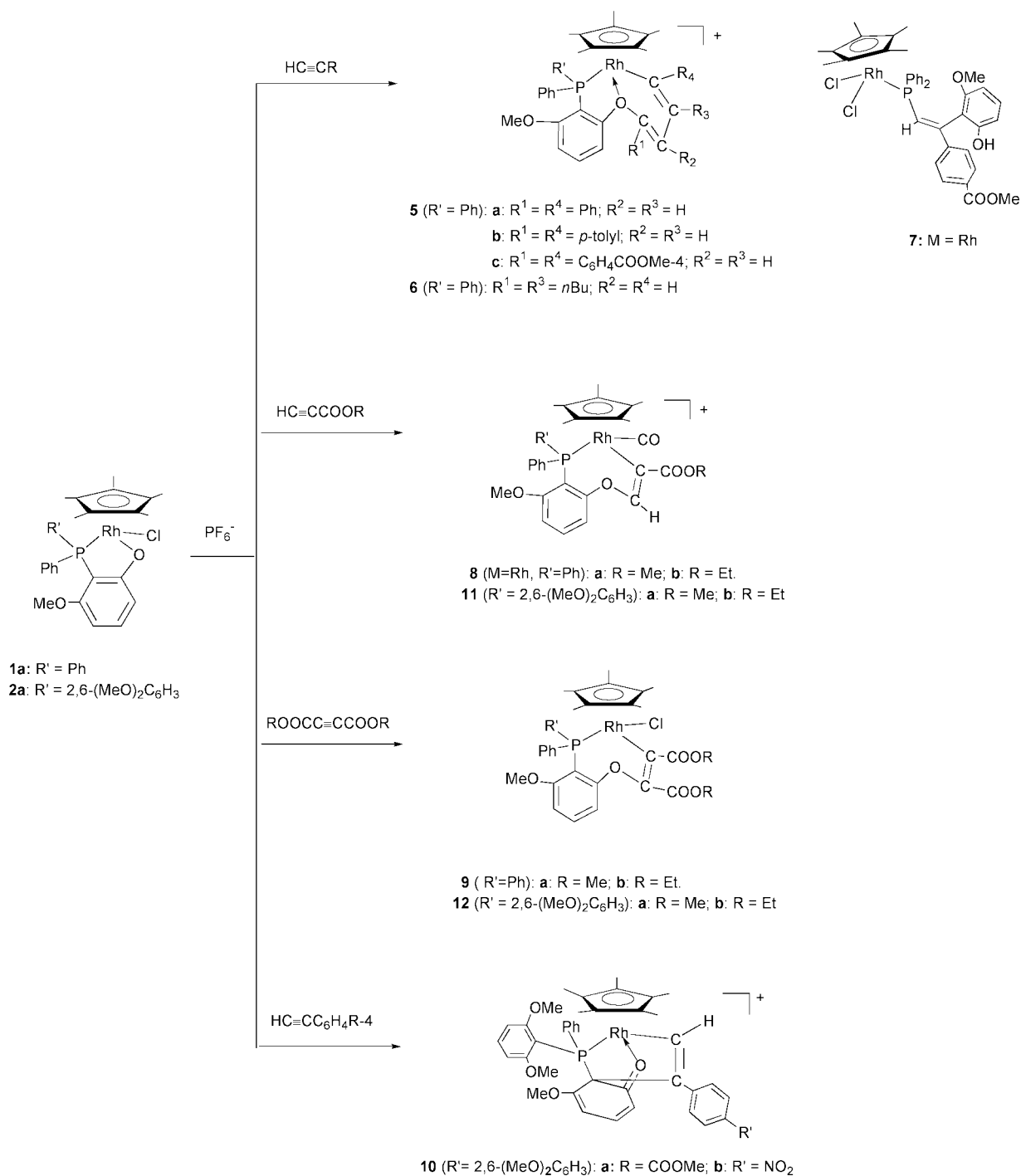


Fig. 5 Molecular structure for the complex cation of **5c**; the PF_6 cation was omitted for clarity and thermal ellipsoids are drawn to encompass 50% probability.

The IR spectrum of **7** indicated three characteristic bands at 3285, 1717 and 1605 cm^{-1} , attributable to $\nu(\text{OH})$, $\nu(\text{C}=\text{O})$ and $\nu(\text{C}=\text{C})$, respectively. The ^1H NMR spectrum showed a broad resonance at δ 6.74 due to a hydroxyl proton in addition to three characteristic methyl resonances at δ 1.41 (d), 3.44 (s) and 3.83 (s) due to the presence of pentamethylcyclopentadienyl, methoxy and methoxycarbonyl groups, respectively. The signal at δ 6.74 disappeared by addition of D_2O . There were no signs of a PF_6 group in the IR and $^{31}\text{P}\{^1\text{H}\}$ NMR spectra, suggesting that the complex was neutral. The structure was confirmed by X-ray analysis and has been reported in the communication.¹⁹ As expected, the molecule is neutral and the rhodium atom is surrounded by two chlorine atoms and one phosphorus atom. *Cis*-insertion of 1-alkyne into the P– C_{ipso} bond of the phosphine ligand occurred, accompanied by the cleavage of an Rh–O bond. In order to examine the origin of the chlorine atoms, reaction in MeOH was carried out. The fact that the only isolable complex is **5c** indicated that the chlorine atom in **7** originated from dichloromethane.

Complex **1a** reacted readily with an excess of $\text{HC}\equiv\text{CCOOMe}$ under similar conditions, giving yellow orange crystals of $[\text{Cp}^*\text{-Rh}(\text{CO})\{\text{PPh}_2(\text{C}_6\text{H}_3-2-(\text{MeO})-6-(\text{OCH}=\text{C}(\text{COOMe}))\}]\text{PF}_6$ **8a**. IR bands at 2060 and 1699 cm^{-1} were assigned to terminal CO and carbomethoxy groups, respectively. The presence of



Scheme 2 Reactions of [Cp*RhCl(MDMPP-*P,O*)] **1a** and [Cp*RhCl(BDMPP-*P,O*)] **2a** with alkynes in the presence of PF₆⁻ anions; PF₆⁻ anions are omitted for clarity.

a PF₆⁻ anion was confirmed by a ν(PF) band at 837 cm⁻¹ in the IR spectrum and a septet at δ -143.9 in the ³¹P{¹H} NMR spectrum. The ¹H NMR spectrum exhibited three characteristic bands at δ 1.54 (d), 3.16 (s) and 3.76 (s), assigned to Cp*, methoxy, and carbomethoxy protons, respectively. The ³¹P{¹H} NMR spectrum showed a signal at δ 3.12 as a doublet. X-Ray analysis revealed that the Rh atom is surrounded by a CO and a P-C bidentate ligand formed by an insertion of methyl propiolate into the rhodium-oxygen σ-bond (Fig. 6). The carbon atom bearing the carbomethoxy group occupied a rhodium site regioselectively as a result of the polarity of the Rh-O and C≡C bonds. A similar complex **8b** was obtained by reaction with HC=CCOOEt. In order to examine the origin of the carbonyl ligand, the reaction was carried out in THF and gave **8a** in high yield, suggesting that the CO group originates from propiolate. Abstraction of CO from the ester groups is quite rare, although Ni(CO)(PPh₃),²² from the reaction of

Ni(cod)₂ with triphenylphosphine and phenyl propionate, and Rh(OAr)(CO)L₂²³ from MeCOOAr and RhHL₄ (L = phosphine), have been documented.

Reactions with internal alkynes such as MeC≡CPh and ROOCC≡CCOOR (R = Me, Et) were carried out in the presence of NaPF₆. The former failed to react, whereas the latter produced reddish orange complexes (**9a**: R = Me; **9b**: R = Et) formulated as [Cp*RhCl{PPh₂(C₆H₃-2-(MeO)-6-(OC(COOR)=C(COOR))))]. Mass spectrometry revealed the masses of **9a** and **9b** to be *m/z* 709 and 737, respectively, calculated on the basis of the loss of a CO molecule from the molecular peaks. The IR spectrum of **9b** showed two bands at 1705 and 1589 cm⁻¹ for a carbonyl group and a C-C double bond, respectively. However, there were no bands at *ca.* 840 cm⁻¹ attributable to the PF₆⁻ group. In the ¹H NMR spectrum, two methylene protons of two COOEt groups gave rise to multiplets at δ 4.03 and 4.18. Each multiplet was observed as a

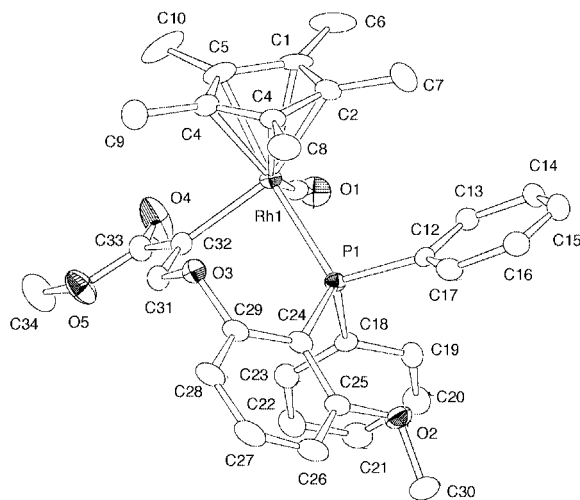


Fig. 6 Molecular structure for the complex cation of **8a**; the PF_6^- cation was omitted for clarity and thermal ellipsoids are drawn to encompass 50% probability.

result of inequivalence of methylene protons CH_aH_b arising from a chiral center of the Rh metal. The methylene protons appeared at δ 1.03 and 1.27 as triplets seemingly, due to same coupling constants ($J_{\text{HH}_a} = J_{\text{HH}_b}$) with each methylene proton, H_a and H_b .

The spectroscopic data suggested that the complex is a seven-membered metallacycle derived from the insertion of $\text{EtOOC}\equiv\text{CCOOEt}$. The proposed structure was confirmed by X-ray analysis.¹⁹ When this reaction was performed without PF_6^- ions, the starting materials were recovered quantitatively. A similar reaction in the presence of NaClO_4 gave **9a**, whereas that in the presence of $[\text{nBu}_4\text{N}]\text{Cl}$ failed to react, suggesting that the presence of large anions such as PF_6^- and ClO_4^- is indispensable for this reaction and an initial extraction of Cl anion is a driving force.

Reactions of $[\text{Cp}^*\text{RhCl}(\text{BDMPP-}P,O)]$ **2a** with alkynes

Reactions of **2a** containing the bidentate bulky phosphine ligand BDMPP-*P,O* with ethynylbenzene or 1-hexyne failed to give isolable complexes. When **2a** in a mixture of CH_2Cl_2 and acetone was treated with 1-ethynylbenzene derivatives bearing an electron-withdrawing substituent such as COOMe or NO_2 in the presence of KPF_6 at room temperature, complexes **10** with empirical formulae $[\text{Cp}^*\text{Rh}(\text{BDMPP-}P,O)(\text{HC}\equiv\text{CC}_6\text{H}_4\text{R-4})](\text{PF}_6)$ (**a**: $\text{R} = \text{COOMe}$, **b**: $\text{R} = \text{NO}_2$) as determined from elemental analyses and FAB mass spectroscopy were generated.

It was confirmed by X-ray analysis of **10b** that the structure contains five- and six-membered rings derived from an unprecedented transannular addition of 1-alkyne between the Rh atom and the *ipso*-carbon atom of the phosphine ligand, and subsequent transformation of the O donor from a phenoxide to an ether coordination (Fig. 7). The IR spectra showed bands at 1715 and 1630 cm^{-1} due to methoxycarbonyl and ketone groups, respectively, for **10a**, and at 1628 cm^{-1} due to a ketone group for **10b**. The ^1H NMR spectra showed three methoxy groups at δ *ca.* 3.0(s), 3.1(bs) and 3.5(bs) for **10a** and **10b**, and a further peak due to a methoxycarbonyl group at δ 3.84(s) for **10a**. A remarkable feature is that the $^{31}\text{P}\{^1\text{H}\}$ NMR doublets showed large downfield shifts (δ *ca.* 140).

Reactions of **2a** with $\text{HC}\equiv\text{CCOOR}$ ($\text{R} = \text{Me}, \text{Et}$) in the presence of KPF_6 at room temperature led to an insertion of 1-alkyne into the Rh–O σ -bond to give the seven-membered complexes $[\text{Cp}^*\text{Rh}(\text{CO})\{P\text{Ph}(\text{C}_6\text{H}_3\text{-}2,6\text{-(MeO)}_2)(\text{C}_6\text{H}_3\text{-}2\text{-(MeO)-}6\text{-(OCH=C(COOR))})\}](\text{PF}_6)$ **11** (**a**: $\text{R} = \text{Me}$; **b**: $\text{R} = \text{Et}$). The IR spectra showed two characteristic bands at *ca.* 2060 and 1690 cm^{-1} due to terminal CO and methoxycarbonyl groups, respectively. The ^1H NMR spectra showed the presence of three

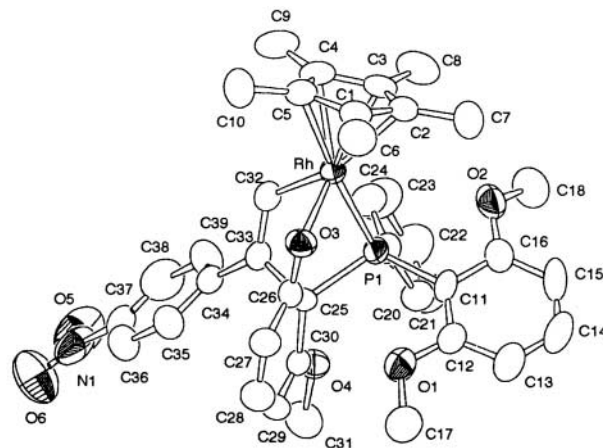


Fig. 7 Molecular structure for the complex cation of **10b**·3H₂O; the PF_6^- cation and H₂O molecules were omitted for clarity and thermal ellipsoids are drawn to encompass 30% probability.

methoxy groups. X-Ray analysis of **11a** revealed that the molecule contains a CO group and a (P,C) bidentate ligand resulting from a regioselective insertion of 1-alkyne into the Rh–O bond (Fig. 8). The carbon atom bearing the carbometh-

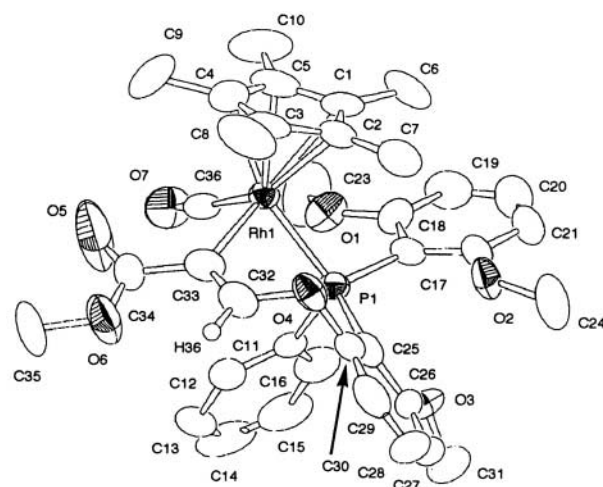


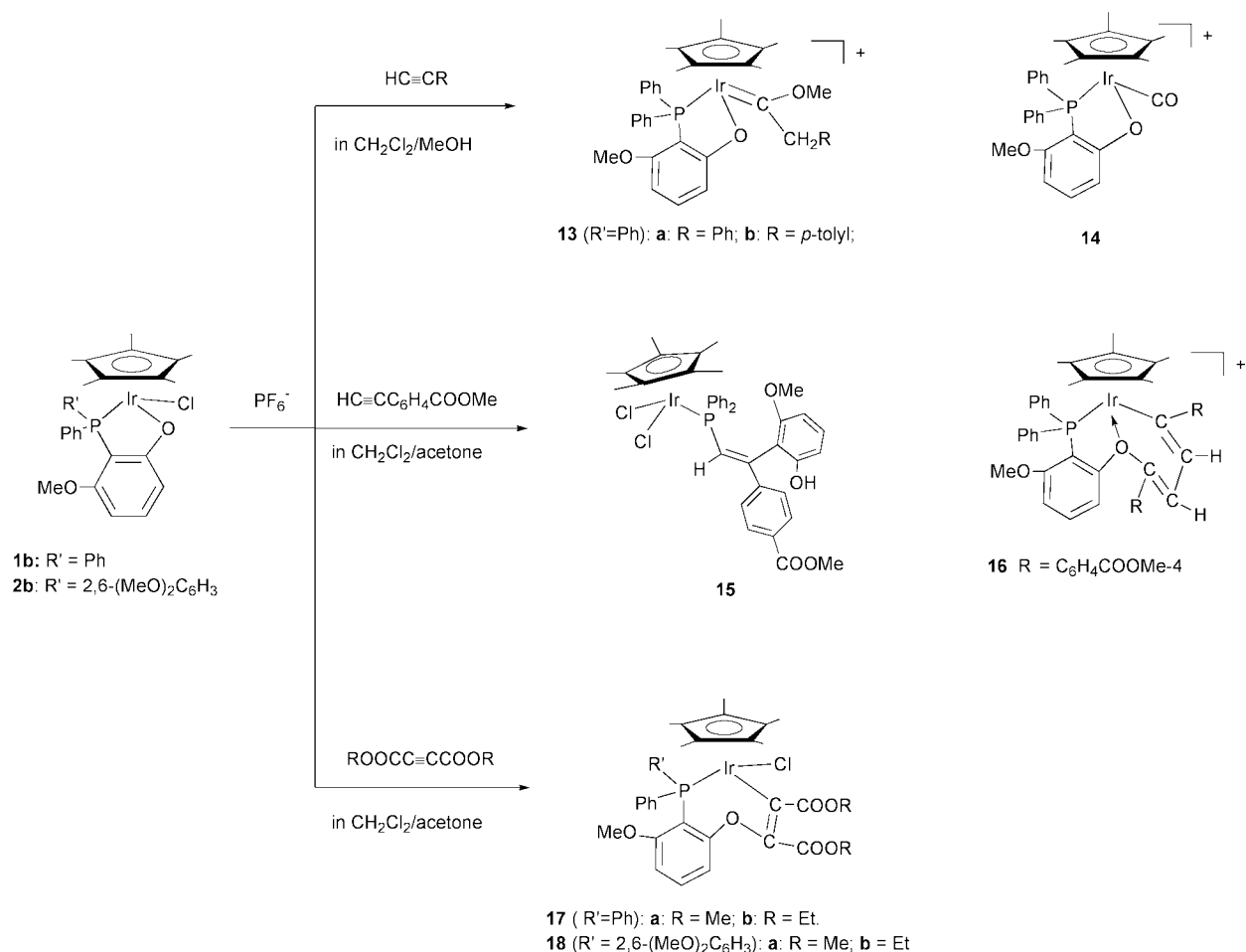
Fig. 8 Molecular structure for the complex cation of **11a**; the PF_6^- cation was omitted for clarity and thermal ellipsoids are drawn to encompass 50% probability.

oxy group is connected to the Rh atom as well as that in **8**. The $^{31}\text{P}\{^1\text{H}\}$ NMR doublets appeared at δ *ca.* –13, at higher fields than those (δ *ca.* 3.2) for **8**.

Acetylene dicarboxylate was treated with **2a** in the presence of KPF_6 at room temperature, leading to an insertion into the Rh–O bond and yielding reddish orange complexes, $[\text{Cp}^*\text{RhCl}\{P\text{Ph}(\text{C}_6\text{H}_3\text{-}2,6\text{-(MeO)}_2)(\text{C}_6\text{H}_3\text{-}2\text{-(MeO)-}6\text{-(OC(COOR)=C(COOR))})\}](\text{PF}_6)$ (**12a**: $\text{R} = \text{Me}$; **12b**: $\text{R} = \text{Et}$) (Fig. 9). The IR spectra showed a band at *ca.* 1705 cm^{-1} due to the C–O double bond. The chemical shift of the coordinated P atom in the $^{31}\text{P}\{^1\text{H}\}$ NMR spectra appeared at δ *ca.* –2.0 as doublets appearing at higher fields than those (δ *ca.* 10) for **9**.

Reactions of $[\text{Cp}^*\text{IrCl}(\text{MDMPP-}P,O)]$ **1b** or $[\text{Cp}^*\text{IrCl}(\text{BDMPP-}P,O)]$ **2b** with alkynes

Overall reactions for iridium complexes are depicted in Scheme 3. Reaction of **1b** with $\text{HC}\equiv\text{CR}$ ($\text{R} = \text{Ph}, p\text{-Tolyl}$) in a mixture of CH_2Cl_2 and MeOH was carried out in the presence of KPF_6 , giving the carbene complexes **13**, $[\text{Cp}^*\text{Ir}(\text{MDMPP-}P,O)\{\text{C}(\text{OMe})\text{CH}_2\text{R}\}](\text{PF}_6)$ (**a**: $\text{R} = \text{Ph}$; **b**: $\text{R} = p\text{-Tolyl}$) as main products and carbonyl complex **14** $[\text{Cp}^*\text{Ir}(\text{MDMPP-}P,O)(\text{CO})](\text{PF}_6)$ as a by-product, unlike the rhodium complexes. Complex **14** was confirmed as a product derived from



Scheme 3 Reactions of [Cp*IrCl(MDMPP-*P,O*)] **1b** and [Cp*IrCl(BDMPP-*P,O*)] **2b** with alkynes in the presence of PF₆⁻ anions; PF₆⁻ anions are omitted for clarity.

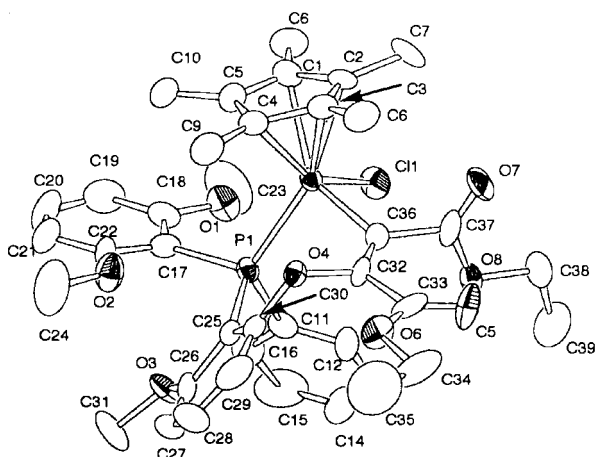


Fig. 9 Molecular structure for the complex cation of **12b**; thermal ellipsoids are drawn to encompass 50% probability.

water in MeOH.²⁴ Carbene structures were confirmed by X-ray analysis of **13a** (Fig. 10).

Reaction of **1b** with HC≡CC₆H₄COOMe-4 proceeded in a similar way to the rhodium analog, forming two complexes; a P–C insertion product **15** Cp*IrCl₂[PPh₂{CH=C(C₆H₄-4-COOMe)(C₆H₃-2-(MeO)-6-(OH))}] and a head-to-head double insertion product **16** [Cp*Ir{PPh₂(C₆H₃-2-(MeO)-6-(OC(C₆H₄-4-COOMe)=CHCH=C(C₆H₄-4-COOMe)))](PF₆). The IR spectrum of **15** showed two characteristic bands at 3312 and 1717 cm⁻¹, due to the OH and C=O double bonds. The ¹H NMR spectrum showed four resonances at δ 1.44 (d), 3.45 (s), 3.84 (s) and 6.64 (bs) due to Cp*, MeO, COOMe and OH protons, respectively. The IR spectrum of **16** showed bands at

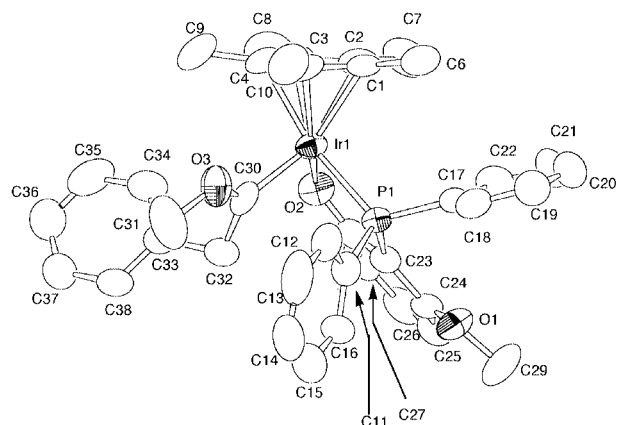


Fig. 10 Molecular structure for the complex cation of **13a**; the PF₆⁻ cation was omitted for clarity and thermal ellipsoids are drawn to encompass 50% probability.

1721 and 843 cm⁻¹ for ν(C=O) and ν(PF₆) groups, respectively. The ¹H NMR spectrum showed resonances at δ 3.67 due to a methoxy group and at δ 3.89 and 3.90 due to two methoxy-carbonyl groups.

Complex **1b** reacted readily with ROCC≡CCOOR (R = Me, Et) in the presence of KPF₆ to produce insertion products **17**, [Cp*IrCl{PPh₂(C₆H₃-2-(MeO)-6-(OC(COOR)=C(COOR)))}] (a: R = Me; b: R = Et). A similar insertion reaction occurred for **2b**, giving **18** [Cp*IrCl{PPh(C₆H₃-2,6-(MeO)₂)(C₆H₃-2-(MeO)-6-(OC(COOR)=C(COOR)))}] (a: R = Me; b: R = Et). The IR spectra of **17** and **18** showed a band at ca. 1700 cm⁻¹ due to ν(CO). In the ¹H NMR spectra the methoxy protons appeared at δ ca. 3.2 for **17** and at δ ca. 3.0, 3.2 and 3.6 for **18**, showing the

NMR patterns similar to the rhodium analogs (**9** and **12**). In the $^{31}\text{P}\{^1\text{H}\}$ NMR spectra the chemical shift values (δ ca. -24) of the coordinated P atoms in **17** showed downfield shifts compared to those (δ ca. -36) of **18**. A similar trend has been observed in rhodium complexes **9** and **12** (*vide supra*). Finally the detailed structures were confirmed by X-ray analyses of **18a** and **18b** (Fig. 11 and 12).

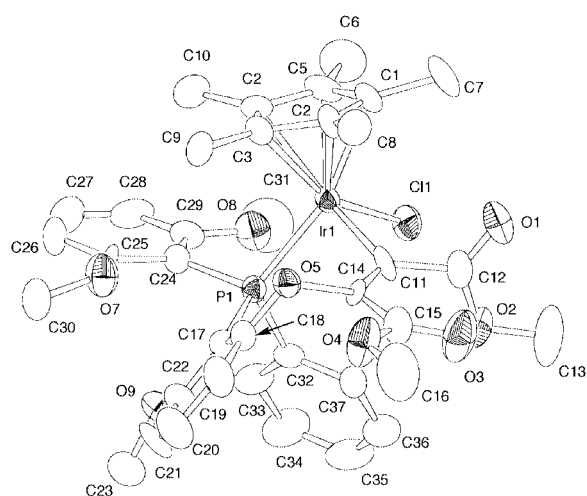


Fig. 11 Molecular structure for the complex cation of **18a**; thermal ellipsoids are drawn to encompass 50% probability.

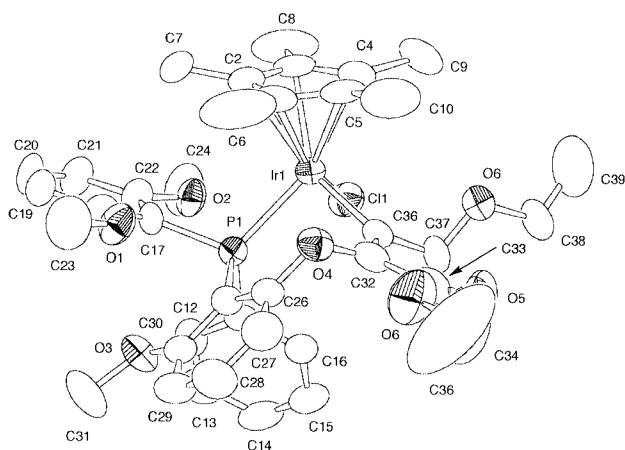


Fig. 12 Molecular structure for the complex cation of **18b**; thermal ellipsoids are drawn to encompass 50% probability.

Reactions of **9** and **14**

When complex **9** was treated with xylyl (Xyl) or mesityl (Mes) isocyanide in the presence of KPF_6 or $\text{Ag}(\text{OTf})$, a substitution reaction occurred readily to produce **19** $[\text{Cp}^*\text{Rh}\{\text{PPh}_2(\text{C}_6\text{H}_3-2-(\text{MeO})-6-(\text{OC}(\text{COOR})=\text{C}(\text{COOR}))\})\}(\text{CNR}')\text{X}]$ ($\text{R} = \text{Me}$ (**a**), Et (**b**); $\text{R}' = \text{Xyl}$ (**c**), Mes (**d**); $\text{X} = \text{PF}_6$ (**e**), OTf (**f**)) (Scheme 4). The IR spectra showed bands at ca. 2160 and 1720 cm^{-1} attributable to isocyanide and carboalkoxy groups, respectively. The ^1H NMR spectra of $[\text{Cp}^*\text{Rh}\{\text{PPh}_2(\text{C}_6\text{H}_3-2-(\text{MeO})-6-(\text{OC}(\text{COOMe})=\text{C}(\text{COOMe}))\})\}(\text{CNR}')\text{X}]$, **19ace** ($\text{R}' = \text{Xyl}$; $\text{X} = \text{PF}_6$), **19acf** ($\text{R}' = \text{Xyl}$; $\text{X} = \text{OTf}$) and **19adf** ($\text{R}' = \text{Mes}$; $\text{X} = \text{OTf}$), showed two singlets at δ ca. 3.8 due to the methoxycarbonyl groups. Those of $[\text{Cp}^*\text{Rh}\{\text{PPh}_2(\text{C}_6\text{H}_3-2-(\text{MeO})-6-(\text{OC}(\text{COOEt})=\text{C}(\text{COOEt}))\})\}(\text{CNR}')\text{X}]$, **19bef** ($\text{R}' = \text{Xyl}$) and **19bdf** ($\text{R}' = \text{Mes}$), showed two triplets at δ ca. 1.3 due to the methyl groups of esters. Methylene protons appeared at δ ca. 4.2 as a quartet, probably due to accidental degeneracy of chemical shifts. The $^{31}\text{P}\{^1\text{H}\}$ NMR spectra showed a doublet at δ ca. 7.0 . It was confirmed by X-ray analysis of **19bcf** that the rhodium atom was surrounded by one P and two C atoms (Fig. 13). A similar reaction of **9a** with carbon monoxide was

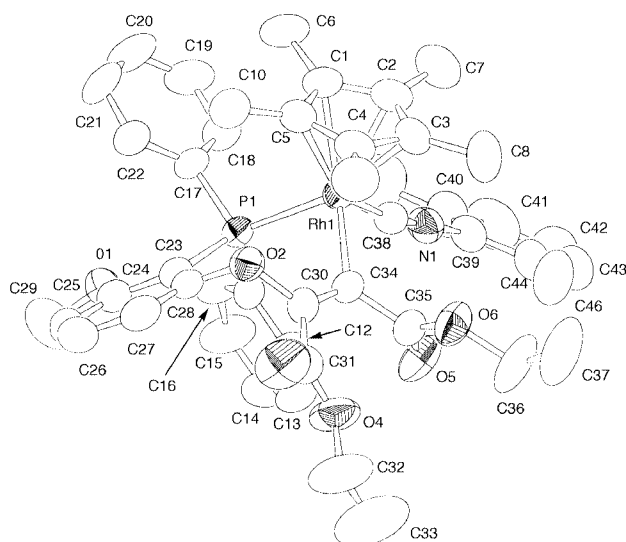


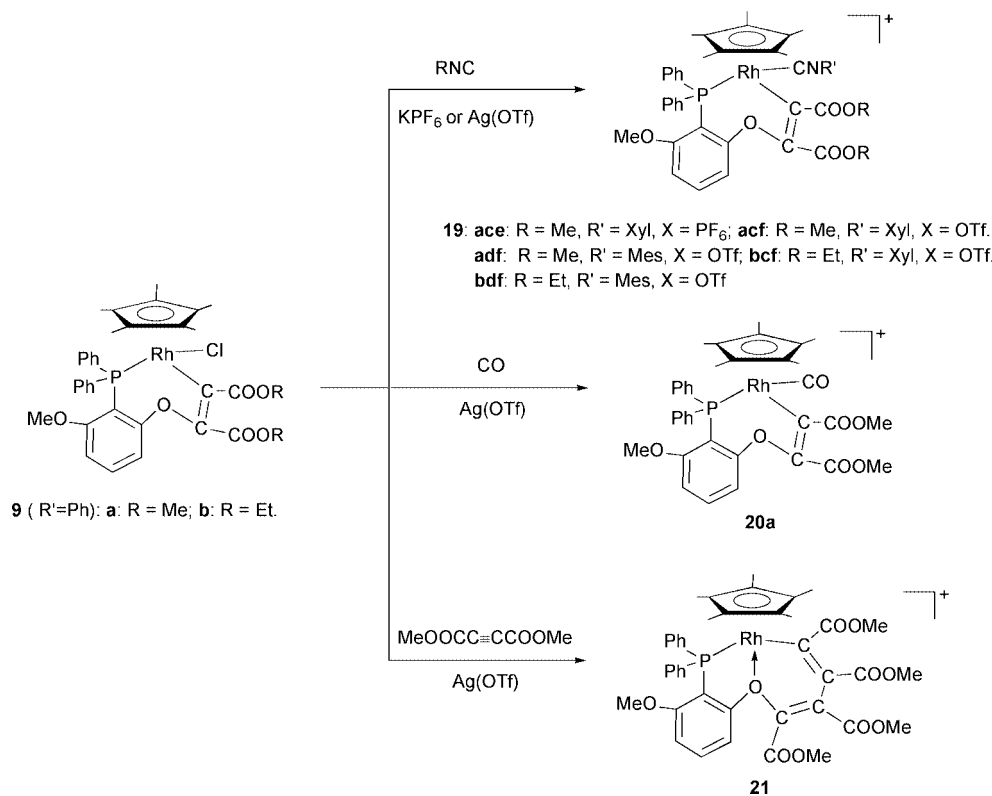
Fig. 13 Molecular structure for the complex cation of **19bcf**; the PF_6 cation was omitted for clarity and thermal ellipsoids are drawn to encompass 50% probability.

carried out in the presence of $\text{Ag}(\text{OTf})$ to generate $[\text{Cp}^*\text{Rh}\{\text{PPh}_2(\text{C}_6\text{H}_3-2-(\text{MeO})-6-(\text{OC}(\text{COOMe})=\text{C}(\text{COOMe}))\})\}(\text{CO})\text{-(OTf)}]$ **20a** in high yield (Scheme 4). The IR spectrum showed bands at 2068 cm^{-1} for a CO ligand and 1715 cm^{-1} for the carbonyl groups.

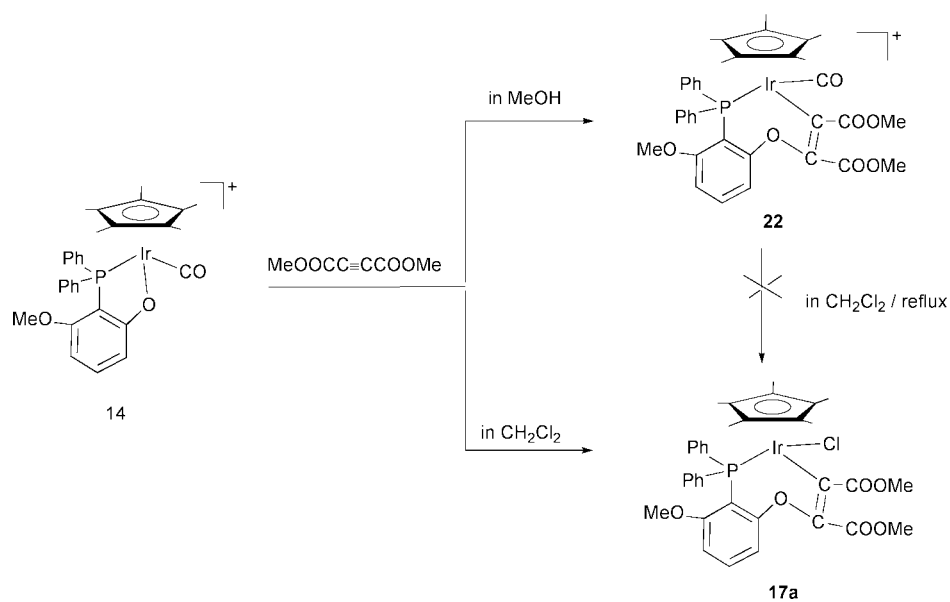
In an attempt to examine coordination ability between ligands, the substitution reactions of **19** or **20a** with another ligand were carried out. Carbonyl complex **20a** reacted readily with 10 equiv. of isocyanide to form corresponding isocyanide complexes **19acf** and **19adf** quantitatively, however, isocyanide complexes failed to react with CO. The coordination ability of isocyanide is stronger than that of CO. No ligand exchange between the isocyanide complex and another isocyanide was observed spectroscopically.

When **9a** and $\text{MeOCC}\equiv\text{CCOOMe}$ was treated with $\text{Ag}(\text{OTf})$ in a mixture of MeOH and CH_2Cl_2 , orange crystals **21** with an empirical formula of $[\text{Cp}^*\text{Rh}(\text{MDMPP-}P,O)(\text{MeOCC}\equiv\text{CCOOMe})_2](\text{OTf})$ from the elemental analysis was generated. Mass spectrometry revealed the mass to be m/z 828 ($[\text{M} - 1]^+$) ($\text{M} = \text{a cationic part}$). The IR spectrum showed $\nu(\text{C}=\text{O})$ bands at 1732 and 1709 cm^{-1} . In the ^1H NMR spectrum, six methyl protons consisting of a doublet and five sharp singlets appeared at δ 1.48 (d), 2.79 , 3.44 , 3.55 , 3.92 and 4.05 , showing that two resonances at δ 1.48 (d) and 2.79 are assignable to Cp^* and methoxy protons, respectively. Other resonances are due to carbomethoxy protons, suggesting the presence of four kinds of methoxycarbonyl groups. The $^{31}\text{P}\{^1\text{H}\}$ NMR spectrum showed a doublet at δ 35.3 ($J_{\text{RHP}} = 148\text{ Hz}$). From these spectroscopic data, the complex is assumed to be a double insertion product of acetylene dicarboxylate into the $\text{Rh}-\text{C}$ bond (Scheme 4). Analogously, complex **21** was generated directly from the reaction of **1a** with $\text{MeOCC}\equiv\text{CCOOMe}$ in the presence of $\text{Ag}(\text{OTf})$.

Reaction of **14** with $\text{MeOCC}\equiv\text{CCOOMe}$ in a mixture of MeOH and CH_2Cl_2 at reflux, led to an insertion of alkyne into the $\text{Ir}-\text{O}$ bond to give **17a** and $[\text{Cp}^*\text{Ir}(\text{CO})\{\text{PPh}_2(\text{C}_6\text{H}_3-2-(\text{MeO})-6-(\text{OC}(\text{COOMe})=\text{C}(\text{COOMe}))\})\}](\text{PF}_6)$ **22**. In order to examine the origin of the Cl atom, the reactions in MeOH or CH_2Cl_2 were carried out. The former gave **22** and the latter gave **17a** exclusively, showing that origin of the Cl atom was derived from dichloromethane (Scheme 5). When **22** was refluxed in CH_2Cl_2 , the starting complex was recovered quantitatively. These results suggest that the route $\text{14} \rightarrow \text{22} \rightarrow \text{17a}$ can be ruled out for the formation of **17a**. Complex **17a** was formed by an initial formation of **1b** arising from an extraction of chlorine anion from CH_2Cl_2 and a subsequent insertion of $\text{MeOCC}\equiv$



Scheme 4 Reactions of **9** with Lewis bases or $\text{MeOOC}\equiv\text{CCOOMe}$; PF_6 or TfO anions are omitted for clarity.



Scheme 5 Reactions of $[\text{Cp}^*\text{Ir}(\text{CO})(\text{MDMPP-}P,O)](\text{PF}_6)$ with $\text{MeOOC}\equiv\text{CCOOMe}$ in MeOH or CH_2Cl_2 ; PF_6 anions are omitted for clarity.

CCOOMe into the $\text{Ir}-\text{O}$ bond of **1b**. Complex **22** was formed directly by an insertion of alkyne into the $\text{Ir}-\text{O}$ bond of **14**.

Pathways for the formation of insertion complexes

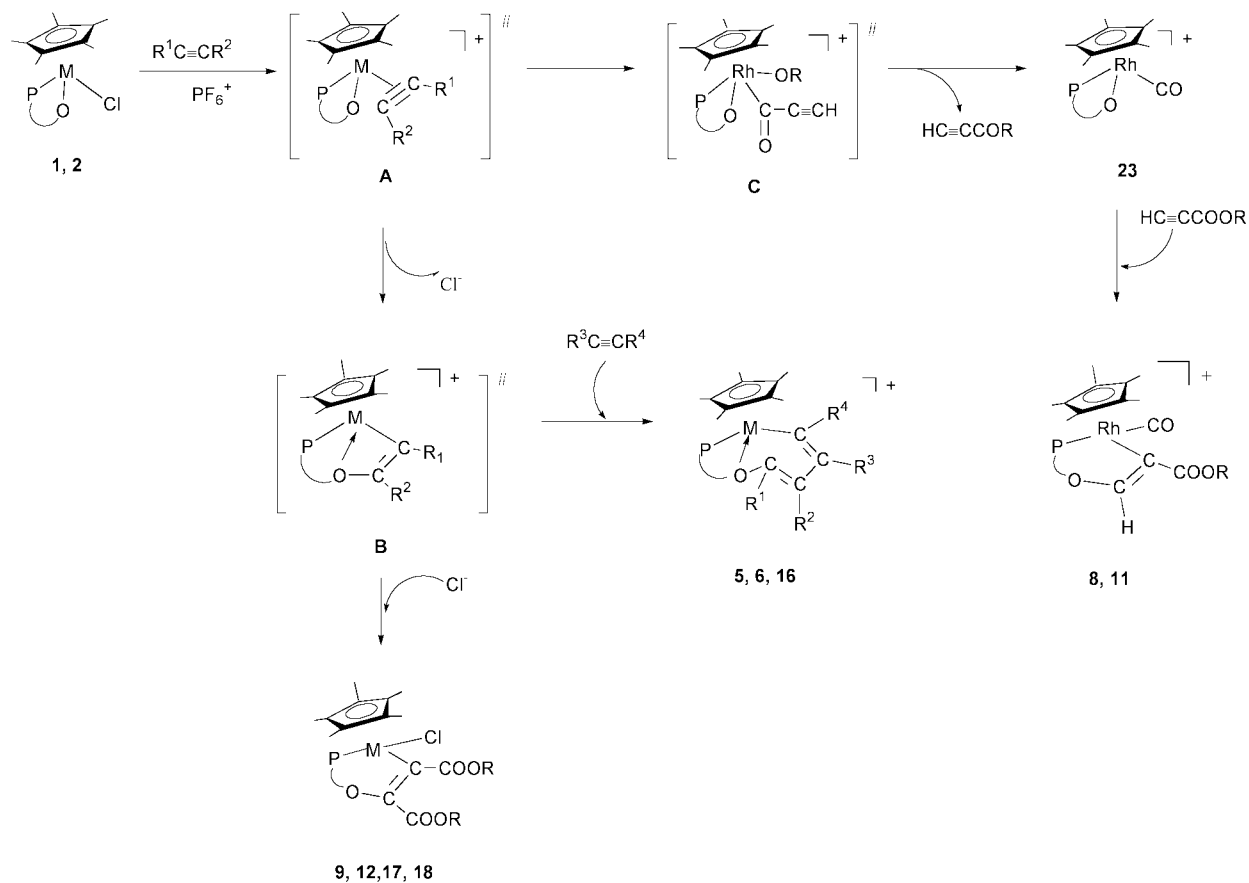
A possible route for the insertion of alkyne into the metal–oxygen bond is depicted in Scheme 6. Initially, the reaction consists of the usual substitution of alkyne to form an intermediate **A**. An insertion of alkyne into the metal–oxygen bond gives an intermediate **B**, and a nucleophilic attack of a Cl^- anion on the intermediate **B** produces **9**, **12**, **17** or **18**. The double-insertion products (**5**, **6** or **16**) are generated by the regioselective insertion of a second alkyne into the metal–carbon bond of the intermediate **B**.

An intermediate **C** is formed by an oxidative addition of ester to the rhodium metal, accompanied by an elimination of

$\text{HC}\equiv\text{COR}$, giving the carbonyl complex **23**, $[\text{Cp}^*\text{Rh}(\text{CO})\{\text{PPh}_2(\text{C}_6\text{H}_3\text{-}2\text{-(MeO)-}6\text{-}O)\}](\text{PF}_6)$. Finally, complex **8** or **11** is formed by the insertion of propiolate into the $\text{Rh}-\text{O}$ bond of the carbonyl complex. The final process was confirmed by the facts that **23** prepared independently¹² reacted readily with $\text{HC}\equiv\text{CCOOMe}$ to give **8a** and the reaction of the iridium complex **14** with $\text{MeOOC}\equiv\text{CCOOMe}$ in MeOH gave the insertion product **22** (Scheme 5). The formation of $\text{HC}\equiv\text{COEt}$ and **8b** was confirmed by monitoring the reaction of **1a** and $\text{HC}\equiv\text{CCOOEt}$ by means of NMR spectroscopy. As yet, no intermediate **B** has been isolated because of the instability of the four-membered ring structure.

Molecular structures

Since perspective drawings, selected bond lengths and angles of **5a**, **7**, and **9b** have already been reported in the literature,^{19,20}



Scheme 6 Possible pathway for the insertion reaction of alkynes (PO = $PPh_2(C_6H_3-6-(MeO)-2-O)$ or $PPh\{C_6H_3-2,6-(MeO)_2\}\{C_6H_3-6-(MeO)-2-O\}$).

Table 1 Selected bond lengths (Å) and angles (°) for $[Cp^*RhCl(BDMPP-P,O)]$ **2a** and $[Cp^*Rh(TDMPP-P,O,O')]$ **4a**

2a					
Rh(1)–P(1)	2.323(2)	Rh(1)–O(2)	2.050(5)	Rh(1)–Cl(2)	2.390(2)
O(2)–C(16)	1.302(8)	C(11)–C(16)	1.41(1)	P(1)–C(11)	1.811(7)
P(1)–Rh(1)–O(2)	83.0(1)	P(1)–Rh(1)–Cl(1)	87.30(7)	O(2)–Rh(1)–Cl(1)	89.5(2)
Rh(1)–O(2)–C(16)	120.7(5)	O(2)–C(16)–C(11)	123.1(6)	P(1)–C(11)–C(16)	113.7(5)
Rh(1)–P(1)–C(11)	99.4(3)				
4a					
Rh(1)–P(1)	2.274(2)	Rh(1)–O(1)	2.065(5)	Rh(1)–O(5)	2.068(5)
O(1)–C(16)	1.334(8)	C(11)–C(16)	1.395(9)	P(1)–C(11)	1.811(7)
O(5)–C(31)	1.306(8)	C(26)–C(31)	1.414(9)	P(1)–C(26)	1.809(6)
P(1)–Rh(1)–O(1)	83.3(1)	P(1)–Rh(1)–O(5)	80.9(1)	O(1)–Rh(1)–O(5)	88.0(2)
Rh(1)–O(1)–C(16)	119.4(4)	O(1)–C(16)–C(11)	121.8(6)	P(1)–C(11)–C(16)	114.6(5)
Rh(1)–P(1)–C(11)	100.6(2)	Rh(1)–O(5)–C(31)	120.7(4)	O(5)–C(31)–C(26)	121.5(6)
P(1)–C(26)–C(31)	111.7(5)	Rh(1)–P(1)–C(26)	101.2(2)		

their structures were omitted here. However, the structure of **10b** is discussed because of brief description in literature.²⁰

Crystal structures of 2a and 4a. Perspective drawings of **2a** and **4a** with atomic numbering schemes are given in Figs. 1 and 2, respectively, and selected bond lengths and angles are listed in Table 1. The molecule of **2a** has two chiral centers (Rh and P atoms). The priority order of the ligands is $Cp^* > Cl > P > O$ for a metal center and $Rh > 2-O-6-(MeO)C_6H_3 > 2,6-(MeO)_2C_6H_3 > Ph$ for a P atom. Fig. 1 shows that the molecule is a $Rh_RP_R/Rh_S P_S$ pair. Complex **4a** has a (P,O,O') tridentate ligand constructed by two five-membered rings. The Rh–P bond length of 2.323(2) Å for **2a** is longer by 0.05 Å than that for **4a**. The P–Rh–O bite angles of both complexes are *ca.* 82°, comparing well with those of iridium and ruthenium complexes.^{10–12}

Structures of 5b, 5c and 6. Perspective drawings of **5b**, **5c** and **6** with atomic numbering schemes are given in Fig. 3–5, and

selected bond lengths and angles are listed in Tables 2 and 3. All complexes consist of two metallacycles derived from a double insertion of alkyne and a transformation of the O donor from a phenoxide to an ester coordination, and all are constructed from five- and six-membered rings shared by a Rh atom, derived in **5** from a head-to-head double insertion of the alkyne and in **6** from a head-to-tail double insertion product. The Rh–P bond lengths of **5** and **6** are in the range 2.268–2.300 Å, similar to that of **1a**,¹² whereas the average Rh–O coordination bond length is 2.218 Å, being *ca.* 0.15 Å longer than that of **1a**, as expected for ether coordination as opposed to a phenoxide. The P–Rh–O bite angles of the five-membered ring were 80°, and the O–Rh–C bite angles of the six-membered ring are in the range 80–81°. These bite angles are independent of the ring size. The P–Rh–C bond angles are wider by *ca.* 10° than those of five- and six-membered rings. The average length of two double bonds in the metallacyclohexadiene rings is *ca.* 1.33 Å, being usual C–C double bonds.

Table 2 Selected bond lengths (Å) and angles (°) for [Cp*Rh{PPh₂(C₆H₃-2-(MeO)-6-(OC(Tolyl)=CHCH=C(Tolyl)))](PF₆) **5b** and [Cp*Rh{PPh₂(C₆H₃-2-(MeO)-6-(OC(C₆H₄-4-COOMe)=CHCH=C(C₆H₄-4-COOMe)))](PF₆) **5c**

5b					
Rh(1)–P(1)	2.30(1)	Rh(1)–O(2)	2.21(2)	Rh(1)–C(47)	2.14(4)
O(2)–C(44)	1.49(4)	C(44)–C(45)	1.35(4)	C(45)–C(46)	1.41(4)
C(46)–C(47)	1.38(5)	P(1)–C(23)	1.87(4)	C(23)–C(28)	1.38(4)
O(2)–C(28)	1.36(4)				
P(1)–Rh(1)–O(2)	80.0(7)	P(1)–Rh(1)–C(47)	91(1)	O(2)–Rh(1)–C(47)	81(1)
Rh(1)–O(2)–C(28)	121(2)	O(2)–C(28)–C(23)	115(3)	P(1)–C(23)–C(28)	118(3)
Rh(1)–P(1)–C(23)	100(1)	Rh(1)–O(2)–C(44)	115(1)	O(2)–C(44)–C(30)	115(3)
O(2)–C(44)–C(45)	108(3)	Rh(1)–C(47)–C(37)	129(3)	Rh(1)–C(47)–C(46)	111(3)
C(37)–C(47)–C(46)	119(4)	C(28)–O(2)–C(44)	111(2)		
5c					
Rh(1)–P(1)	2.300(3)	Rh(1)–O(2)	2.214(7)	Rh(1)–C(33)	2.06(1)
O(2)–C(30)	1.43(1)	C(30)–C(31)	1.33(2)	C(31)–C(32)	1.45(2)
C(32)–C(33)	1.33(2)	P(1)–C(23)	1.81(1)	C(23)–C(28)	1.37(2)
O(2)–C(28)	1.44(1)				
P(1)–Rh(1)–O(2)	80.2(2)	P(1)–Rh(1)–C(33)	91.1(3)	O(2)–Rh(1)–C(33)	80.8(4)
Rh(1)–O(2)–C(28)	119.3(7)	O(2)–C(28)–C(23)	116.1(10)	P(1)–C(23)–C(28)	119.4(9)
Rh(1)–P(1)–C(23)	102.7(4)	Rh(1)–O(2)–C(28)	119.3(7)	O(2)–C(30)–C(31)	115(1)
C(30)–C(31)–C(32)	125(1)	C(31)–C(32)–C(33)	128(1)	Rh(1)–C(33)–C(32)	118(1)

Table 3 Selected bond lengths (Å) and angles (°) for [Cp*Rh{PPh₂(C₆H₃-2-(MeO)-6-(OC(*n*Bu)CH=C(*n*Bu)=CH)))](PF₆) **6**

Rh(1)–P(1)	2.268(5)	Rh(1)–O(1)	2.23(1)	Rh(1)–C(35)	2.01(2)
O(1)–C(37)	1.46(2)	C(36)–C(37)	1.33(2)	C(34)–C(36)	1.49(3)
C(34)–C(35)	1.30(2)	P(1)–C(23)	1.82(2)	C(23)–C(24)	1.34(2)
O(1)–C(24)	1.45(2)				
P(1)–Rh(1)–O(1)	80.3(3)	P(1)–Rh(1)–C(35)	88.1(6)	O(1)–Rh(1)–C(35)	80.0(6)
Rh(1)–O(1)–C(24)	116.0(10)	Rh(1)–O(1)–C(37)	108.9(10)	C(24)–O(1)–C(37)	117(1)
O(1)–C(24)–C(23)	118(1)	P(1)–C(23)–C(24)	117(1)	Rh(1)–P(1)–C(23)	103.5(6)
O(1)–C(37)–C(36)	115(1)	O(1)–C(37)–C(38)	111(1)	C(34)–C(36)–C(37)	125(1)
C(36)–C(34)–C(35)	122(1)	C(33)–C(34)–C(36)	114(1)	Rh(1)–C(35)–C(34)	124(1)

Table 4 Selected bond lengths (Å) and angles (°) for [Cp*Rh(CO){PPh₂(C₆H₃-2-(MeO)-6-(OCH=C(COOMe)))](PF₆) **8a** and [Cp*Rh(CO){PPh(C₆H₃-2,6-(MeO)₂)(C₆H₃-2-(MeO)-6-(OCH=C(COOMe)))](PF₆)(PF₆) **11a**

8a					
Rh(1)–P(1)	2.349(1)	Rh(1)–C(11)	1.909(6)	Rh(1)–C(32)	2.072(5)
C(11)–O(1)	1.128(6)	C(31)–C(32)	1.309(8)	O(3)–C(31)	1.412(6)
C(24)–C(29)	1.391(8)	P(1)–C(24)	1.816(5)	C(32)–C(33)	1.487(7)
O(4)–C(33)	1.199(7)	O(5)–C(33)	1.337(7)		
P(1)–Rh(1)–C(11)	89.6(2)	P(1)–Rh(1)–C(32)	86.5(1)	C(11)–Rh(1)–C(32)	93.2(2)
Rh(1)–P(1)–C(24)	118.8(2)	P(1)–C(24)–C(29)	123.0(4)	O(3)–C(29)–C(24)	119.9(5)
O(3)–C(31)–C(32)	119.7(5)	Rh(1)–C(32)–C(31)	120.0(4)	Rh(1)–C(11)–O(1)	173.5(5)
11a					
Rh(1)–P(1)	2.364(6)	Rh(1)–C(33)	2.15(2)	Rh(1)–C(36)	2.05(3)
C(36)–O(7)	1.04(3)	C(32)–C(33)	1.32(3)	O(4)–C(32)	1.44(3)
O(4)–C(30)	1.40(3)	P(1)–C(25)	1.89(2)	C(25)–C(30)	1.40(3)
O(5)–C(34)	1.14(3)	O(6)–C(34)	1.29(3)		
P(1)–Rh(1)–C(33)	89.7(7)	P(1)–Rh(1)–C(36)	90.8(7)	C(33)–Rh(1)–C(36)	89.8(10)
Rh(1)–P(1)–C(25)	118.9(9)	P(1)–C(25)–C(30)	120(1)	C(25)–C(30)–O(4)	121(2)
O(4)–C(32)–C(33)	122(2)	Rh(1)–C(33)–C(32)	116(2)	Rh(1)–C(33)–C(34)	122(1)
Rh(1)–C(36)–O(7)	175(2)				

Structures of 8a and 11a. Perspective drawings of **8a** and **11a** with atomic numbering schemes are given in Figs. 6 and 8, respectively, and selected bond lengths and angles are listed in Table 4. The Rh atom is surrounded by a CO ligand and a P–O bidentate ligand derived from the insertion of propiolate into the Rh–O bond. A carbon atom bearing a carbomethoxy group occupies a rhodium site as the result of the polarity of the alkyne. Complex **11a** has two chiral centers. The priority order of the ligands is Cp* > P > CO > C for a Rh center and Rh > 2-O-6-MeOC₆H₃ > 2,6-(MeO)₂C₆H₃ > Ph for a P center. Fig. 8 shows a Rh_RP_R/Rh_SP_S pair. The seven-membered rings of **8a** and **11a** are divided into two planes; Rh(1)O(3)C(31)C(32) and Rh(1)P(1)O(3)C(24)C(29) for **8a**, and Rh(1)O(4)C(32)C(33) and Rh(1)P(1)O(4)C(25)C(30) for **11a**; the dihedral angle of the

former is 74.6(2)° and that of the latter is 69.7(5)°. The smaller angle of **11a** provides a larger space for the 2,6-(MeO)₂C₆H₃ ring. The Rh–P, Rh–C(=CH–) and Rh–CO bond lengths of **11a** are longer than those of **8a**, minimizing steric repulsion between bulky 2,6-dimethoxyphenyl and pentamethylcyclopentadienyl moieties. The C=C double bond lengths are usual. The Rh–C–O bond angles are the usual value of 174°. The angles around the Rh atom containing the P atom in **11a** are wider than those of **8a**, due to the bulkiness of the 2,6-(MeO)₂C₆H₃ (Å) group.

Structures of 12b, 18a and 18b. Perspective drawings of **12b**, **18a** and **18b** with atomic numbering schemes are given in Figs. 9, 11 and 12, respectively. Selected bond lengths and angles are listed in Table 5. The molecule is neutral and consists of a

Table 5 Selected bond lengths (Å) and angles (°) for [Cp*RhCl{PPh(C₆H₃-2,6-(MeO)₂)(C₆H₃-2-(MeO)-6-(OC(COOR)=C(COOR))))] **12b**, [Cp*IrCl{PPh(C₆H₃-2,6-(MeO)₂)(C₆H₃-2-(MeO)-6-(OC(COOMe)=C(COOMe))))] **18a** and [Cp*IrCl{PPh(C₆H₃-2,6-(MeO)₂)(C₆H₃-2-(MeO)-6-(OC(COOEt)=C(COOEt))))] **18b**

12b					
Rh(1)–P(1)	2.344(3)	Rh(1)–Cl(1)	2.402(3)	Rh(1)–C(36)	2.02(1)
C(32)–C(36)	1.35(2)	O(4)–C(32)	1.39(1)	O(4)–C(30)	1.39(1)
C(25)–C(30)	1.40(1)	P(1)–C(25)	1.86(1)	C(32)–C(33)	1.51(2)
C(33)–O(5)	1.19(1)	C(33)–O(6)	1.34(2)	C(36)–C(37)	1.50(2)
C(37)–O(7)	1.17(1)	C(37)–O(8)	1.35(1)		
P(1)–Rh(1)–Cl(1)	95.0(1)	P(1)–Rh(1)–C(36)	89.2(3)	Cl(1)–Rh(1)–C(36)	90.2(3)
Rh(1)–P(1)–C(25)	118.1(4)	P(1)–C(25)–C(30)	123.7(8)	C(25)–C(30)–O(4)	121(1)
O(4)–C(32)–C(36)	120(1)	Rh(1)–C(36)–C(32)	122.4(9)	O(4)–C(32)–C(33)	114(1)
C(32)–C(33)–O(5)	124(1)	C(32)–C(33)–O(6)	111(1)	O(5)–C(33)–O(6)	123(1)
Rh(1)–C(36)–C(37)	117.7(9)	C(32)–C(36)–C(37)	118(1)	O(7)–C(37)–C(36)	123(1)
C(36)–C(37)–O(8)	111(1)	O(7)–C(37)–O(8)	124(1)		
18a					
Ir(1)–P(1)	2.325(2)	Ir(1)–Cl(1)	2.417(3)	Ir(1)–C(11)	2.05(1)
C(11)–C(14)	1.33(1)	O(5)–C(14)	1.40(1)	O(5)–C(18)	1.38(1)
C(17)–C(18)	1.38(1)	P(1)–C(17)	1.874(10)	C(12)–O(1)	1.19(1)
C(12)–O(2)	1.33(1)	C(15)–O(3)	1.22(1)	C(15)–O(4)	1.30(1)
P(1)–Ir(1)–Cl(1)	94.50(9)	P(1)–Ir(1)–C(11)	89.7(3)	Cl(1)–Ir(1)–C(11)	89.1(3)
Ir(1)–P(1)–C(17)	117.0(3)	P(1)–C(17)–C(18)	124.5(7)	C(17)–C(18)–O(5)	121.4(9)
O(5)–C(14)–C(11)	119.6(9)	Ir(1)–C(11)–C(14)	122.0(8)	Ir(1)–C(11)–C(12)	119.1(7)
C(12)–C(11)–C(14)	118.1(10)	O(1)–C(12)–C(11)	122(1)	C(11)–C(12)–O(2)	112.9(9)
O(1)–C(12)–O(2)	124(1)	O(5)–C(14)–C(15)	115.4(9)	C(11)–C(14)–C(15)	123.9(9)
C(15)–C(14)–O(5)	115.4(9)	O(3)–C(15)–O(4)	121(1)	C(14)–C(15)–O(3)	123(1)
O(4)–C(15)–C(14)	115.2(9)				
18b					
Ir(1)–P(1)	2.314(4)	Ir(1)–Cl(1)	2.397(4)	Ir(1)–C(36)	2.08(2)
C(32)–C(36)	1.37(2)	O(4)–C(32)	1.40(2)	O(4)–C(26)	1.40(2)
C(25)–C(26)	1.42(2)	P(1)–C(25)	1.87(1)	C(33)–O(5)	1.16(2)
C(33)–O(6)	1.37(2)	C(37)–O(7)	1.17(2)	C(37)–O(8)	1.37(2)
P(1)–Ir(1)–Cl(1)	93.7(1)	P(1)–Ir(1)–C(36)	89.7(4)	Cl(1)–Ir(1)–C(36)	89.5(5)
Ir(1)–P(1)–C(25)	118.1(5)	P(1)–C(25)–C(26)	123(1)	C(25)–C(26)–O(4)	121(1)
C(26)–O(4)–C(32)	115(1)	O(4)–C(32)–C(36)	119(1)	Ir(1)–C(36)–C(32)	121(1)
O(4)–C(32)–C(33)	119(1)	C(33)–C(32)–C(36)	119(1)	C(32)–C(33)–O(5)	128(2)
C(32)–C(33)–O(6)	107(2)	O(5)–C(33)–O(6)	124(1)	Ir(1)–C(36)–C(37)	120(1)
C(32)–C(36)–C(37)	118(1)	C(36)–C(37)–O(7)	127(1)	O(7)–C(37)–O(8)	125(1)
C(36)–C(37)–O(8)	107(1)				

Table 6 Selected bond lengths (Å) and angles (°) for [Cp*Rh{PPh(C₆H₃-2,6-(MeO)₂)(C₆H₃-1-C(C₆H₄-4-COOMe)-C)-2-(MeO)-6(=O))}(PF₆)₃H₂O]

Rh(1)–P(1)	2.305(2)	Rh(1)–O(3)	2.108(6)	Rh(1)–C(32)	2.017(9)
O(3)–C(26)	1.26(1)	C(25)–C(26)	1.51(1)	P(1)–C(25)	1.946(9)
C(25)–C(30)	1.51(1)	C(26)–C(27)	1.41(1)	C(27)–C(28)	1.35(1)
C(28)–C(29)	1.42(1)	C(29)–C(30)	1.31(1)	C(32)–C(33)	1.34(1)
C(25)–C(33)	1.57(1)				
P(1)–Rh(1)–O(3)	81.1(2)	P(1)–Rh(1)–C(32)	76.2(3)	O(3)–Rh(1)–C(32)	85.5(3)
Rh(1)–P(1)–C(25)	90.1(3)	P(1)–C(25)–C(26)	105.2(6)	C(25)–C(26)–O(3)	118.2(8)
Rh(1)–O(3)–C(26)	118.2(6)	Rh(1)–C(32)–C(33)	120.1(7)	C(32)–C(33)–C(25)	114.5(8)
P(1)–C(25)–C(33)	96.5(6)	O(3)–C(26)–C(27)	122.1(9)		

seven-membered metallacycle derived from the insertion of acetylene dicarboxylate into the metal–O bond. The metal is surrounded by a Cl atom and a P–C bidentate ligand. Figs. 9, 11 and 12 showed that these complexes are Rh_RP_R/Rh_SP_S pairs. The metallacycle is divided into two planes; Rh(1)O(1)C(30)C(31) and Rh(1)P(1)O(1)C(23)C(28) for **9b**,¹⁹ Rh(1)O(4)C(3)C(36) and Rh(1)P(1)O(4)C(25)C(30) for **12b**, Ir(1)O(5)C(11)C(14) and Ir(1)P(1)O(5)C(17)C(18) for **18a** and Ir(1)O(4)C(32)C(36) and Ir(1)P(1)O(4)C(25)C(26) for **18b**; the dihedral angles are 73.4(7), 69.2(5), 69.8(4) and 69.8(5)°, respectively. The fact that the dihedral angles (*ca.* 70°) of complexes bearing sterically bulky phosphine ligand are narrower than that (*ca.* 73°) of **9b** with less bulky phosphine also provides a larger space for the 2,6-(MeO)₂C₆H₃ moiety. The dihedral angles between the plane (M–C–C–O) of four atoms containing metal and O atoms and the planes (O=C–O) of the ester groups are 10–15° and 72–78°, respectively, and those between ester

groups fall in the range 80–90°, minimizing steric hindrance between ester groups.

Structure of 10b. A perspective drawing of **10b** with an atomic numbering scheme is given in Fig. 7, and selected bond lengths and angles are listed in Table 6. The Rh atom is surrounded by a (P, O, C) tridentate ligand derived from a transannular addition of 1-alkyne between the Rh atom and the *ipso*-carbon atom of the phosphine ligand, accompanying the subsequent transformation of the O donor from the phenoxide to the ketone coordination. The change of this bonding mode causes an elongation of 0.056 Å from 2.050 to 2.106 Å in the Rh–O bond lengths. The molecule has three chiral centers. The priority of order of the ligands is Cp* > P > O > C for a Rh center, Rh > *ipso*-C > 2,6-(MeO)₂C₆H₃ > Ph for a P center, and Rh > O > C for an *ipso*-carbon center. Fig. 7 shows that the molecule is a Rh_RP_SC_S/Rh_SP_RC_R pair. The

Table 7 Selected bond lengths (Å) and angles (°) for [Cp*Ir(MDMPP-*P,O*){C(OMe)CH₂Ph}](PF₆) **13a**

Ir(1)–P(1)	2.300(3)	Ir(1)–O(2)	2.103(7)	Ir(1)–C(30)	1.97(1)
C(30)–C(32)	1.56(2)	O(3)–C(30)	1.30(1)	O(2)–C(28)	1.33(1)
C(23)–C(28)	1.40(1)	P(1)–C(23)	1.81(1)		
P(1)–Ir(1)–O(2)	82.4(2)	P(1)–Ir(1)–C(30)	89.5(4)	O(2)–Ir(1)–C(30)	89.5(4)
Ir(1)–P(1)–C(23)	101.1(4)	P(1)–C(23)–C(28)	114.2(8)	C(23)–C(28)–O(2)	121(1)
Ir(1)–O(2)–C(28)	119.6(7)	Ir(1)–C(30)–O(3)	117.3(9)	Ir(1)–C(30)–C(32)	125.7(8)
O(3)–C(30)–C(32)	116(1)				

Table 8 Selected bond lengths (Å) and angles (°) for [Cp*Rh{PPh₂(C₆H₃-2-(MeO)-6-(OC(COOEt)=C(COOEt)))}(CNXyl)](PF₆) **19bcf**

Rh(1)–P(1)	2.350(2)	Rh(1)–C(34)	2.093(8)	Rh(1)–C(38)	1.947(10)
C(30)–C(34)	1.31(1)	O(2)–C(30)	1.413(9)	O(2)–C(28)	1.39(1)
C(23)–C(28)	1.43(1)	P(1)–C(23)	1.811(9)	C(38)–N(1)	1.15(1)
P(1)–Rh(1)–C(34)	87.6(2)	P(1)–Rh(1)–C(38)	92.2(3)	C(34)–Rh(1)–C(38)	94.1(3)
Rh(1)–P(1)–C(23)	118.5(3)	P(1)–C(23)–C(28)	123.3(7)	C(23)–C(28)–O(2)	118.9(8)
O(2)–C(30)–C(34)	120.3(8)	Rh(1)–C(34)–C(30)	118.9(6)	Rh(1)–C(38)–N(1)	172.2(8)
C(38)–N(1)–C(39)	178.7(9)				

carbon atom bearing the 4-substituted phenyl group is connected to the *ipso*-carbon atom as a result of the polarity of the alkyne. The Rh–P length of 2.305(2) Å is not different from those found in related complexes. The Rh(1)–C(32) length of 2.017(9) Å is shorter than that for the complexes described here. The C(32)–C(33) bond length of 1.34(1) Å indicates C–C double bond. The average length of 1.33 Å for the C(27)–C(28) and C(29)–C(30) double bonds is shorter than that of 1.46 Å for the C(25)–C(26), C(25)–C(30), C(26)–C(27) and C(28)–C(29) single bonds, consisting with a cyclohexadiene ring. The C(26)–O(3) length of 1.26(1) Å is a usual double bond value. The P(1)–Rh(1)–O(3) bite angle of 81.1(2)° and P(1)–Rh(1)–C(32) bite angles of 76.2(3)° in the five-membered rings are narrower than the O(3)–Rh(1)–C(32) bite angle (85.5(3)°) of the six-membered ring.

Structure of 13a. A perspective drawing of **13a** with an atomic numbering scheme is given in Fig. 10. Selected bond lengths and angles are listed in Table 7. The Ir(1)–P(1) and Ir(1)–O(2) bond lengths are essentially the same as those in other complexes. The Ir–C(30) bond length of 1.97 Å is *ca.* 0.10 Å shorter than the Ir–C σ -bond length for **18**, showing the presence of the Ir–C carbene bond. The C(30)–O(3) bond length of 1.30 Å is shorter than usual C–O single bond length, suggesting the presence of electron delocalization in the Ir–C(30)–O(2) moiety.

Structure of 19bcf. A perspective drawing of **19bcf** with an atomic numbering scheme is given in Fig. 13, and selected bond lengths and angles are listed in Table 8. The Rh(1)–P(1) bond length of 2.350(2) Å and Rh(1)–C(34) length of 2.093(8) Å are about 0.05 Å longer than the corresponding lengths in the neutral complex **9b**,¹⁹ as a result of the steric demand of the isocyanide ligand. The Rh(1)–C(38) bond length of 1.947(10) Å is shorter than the Rh(1)–C(34) bond length, as a result of different bonding modes. The C(38)–N(1) bond length of 1.15(1) Å is comparable with a usual C–N triple bond length. The Rh(1)–C(38)–N(1) and C(38)–N(1)–C(39) bond angles are nearly linear

Experimental

All syntheses were carried out under a nitrogen atmosphere. Dichloromethane was distilled over CaH₂ and diethyl ether was distilled over LiAlH₄. Isocyanides,²⁵ phosphines²⁶ and pentamethylcyclopentadienyl complexes of rhodium¹² and iridium¹³ were prepared according to the literature. The infrared and electronic absorption spectra were measured on FT/IR-5300 and U-best 30 instruments, respectively. The ¹H NMR spectra were measured at 250 MHz, and ³¹P{¹H} NMR spectra were

measured at 101 MHz using 85% H₃PO₄ as an external reference. Elemental analyses were performed by Analytical Center, Faculty of Pharmaceutical Department, Toho University.

Reaction of [Cp*RhCl₂]₂ with BDMPP

A solution of [Cp*RhCl₂]₂ (1.035 g, 1.67 mmol) and BDMPP (3.21 g, 8.38 mmol) was refluxed in EtOH (10 mL) for 20 h. The solvent was removed and the residue extracted with benzene. After removal of benzene, the residue was chromatographed on deactivated alumina (containing 10% H₂O) using CH₂Cl₂ and ethyl acetate as eluents. The solvent was removed from the reddish brown eluate with CH₂Cl₂ and the residue was washed with diethyl ether to give orange solid **3a** (0.68 g, 34%). The work-up of the eluate with ethylacetate gave orange solid **2a** (1.15 g, 53%). **2a**: ¹H NMR (250 MHz, CDCl₃): δ 1.51 (d, $J_{\text{PH}} = 3.0$ Hz, Cp*, 15H), 3.08 (s, OMe, 3H), 3.25 (s, OMe, 3H), 3.74 (s, OMe, 3H), 5.8–7.5 (m, ArH, 11H). ³¹P NMR (100 MHz, CDCl₃): δ 55.7 (d, $J_{\text{RHP}} = 127$ Hz). Anal. Calc. for C₃₁H₃₅O₄PClRh: C, 58.09; H, 5.50. Found C, 58.10; H, 5.26%. **3a**: UV (CH₂Cl₂): λ_{max} 303 (sh), 235 nm. ¹H NMR (250 MHz, CDCl₃): δ 1.34 (d, $J_{\text{PH}} = 2.5$ Hz, Cp*, 15H), 3.51 (s, OMe, 6H), 5.7–7.7 (m, ArH, 11H). ³¹P NMR (100 MHz, CDCl₃): δ 36.9 (d, $J_{\text{RHP}} = 157.5$ Hz). Anal. Calc. for C₃₀H₃₅O₄PRh: C, 61.02; H, 5.46. Found C, 60.88; H, 5.74%.

Reaction of [Cp*RhCl₂]₂ with TDMPP

A solution of [Cp*RhCl₂]₂ (1.06 g, 1.72 mmol) and TDMPP (442 mg, 1.0 mmol) was stirred in MeOH (10 mL) at room temperature. After 50 h, the solvent was removed under reduced pressure and the residue extracted with benzene. Benzene was removed and the residue was washed with diethyl ether to give orange solid **4** (153 mg, 68%). **4**: UV(CH₂Cl₂): λ_{max} 302, 235 nm. ¹H NMR (250 MHz, CDCl₃): δ 1.45 (d, $J_{\text{PH}} = 2.5$ Hz, Cp*, 15H), 3.42 (s, OMe, 6H), 3.49 (s, OMe, 6H), 5.7–7.6 (m, ArH, 9H). ³¹P NMR (100 MHz, CDCl₃): δ 43.7 (d, $J_{\text{RHP}} = 137.5$ Hz). Anal. Calc. for C₃₂H₃₆O₆PRh: C, 59.08; H, 5.58. Found C, 59.33; H, 5.78%.

Reaction of 1a with ethynylbenzene

To a solution of **1a** (50 mg, 0.086 mmol) and PhC \equiv CH (0.1 mL) in CH₂Cl₂ (15 mL) and acetone (10 mL) was added an excess of NaPF₆ at room temperature. After 4 h, the solvent was removed and the residue was extracted with CH₂Cl₂. The CH₂Cl₂ was removed to give an oily product and the residue was chromatographed on silica gel using CH₂Cl₂-*n*-hexane (1 : 5) as an eluant. Reddish brown eluate was dried and the residue recrystallized from CH₂Cl₂-diethyl ether to give orange crystals of **5a** (27 mg, 35%). IR (Nujol): 1591, 1568, 837 cm⁻¹. UV

(CH₂Cl₂): λ_{\max} ca. 360, 286 nm. ¹H NMR (250 MHz, CDCl₃): δ 1.35 (d, $J_{\text{PH}} = 2.5$ Hz, Cp*, 15H), 3.30 (s, OMe, 3H), 6.3–7.6 (m, CH= and ArH, 25H). ³¹P{¹H} NMR (100 MHz, CDCl₃): δ 36.9 (d, $J_{\text{RHP}} = 157.5$ Hz), –143.8 (septet, $J_{\text{PF}} = 717$ Hz, PF₆[–]). FAB mass (m/z of cationic part): 749 (749.7). Anal. Calc. for C₄₅H₄₃O₂P₂F₆Rh: C, 60.41; H, 4.84. Found C, 60.12; H, 4.83%.

Reddish brown complex **5b** (26 mg, 30%) was prepared by the reaction of **1a** (54.5 mg, 0.095 mmol) with ethynyltoluene (0.2 mL) in the presence an excess of NaPF₆ by a procedure similar to that for **5a**. IR (Nujol): 1591, 1568, 837 cm^{–1}. UV (CH₂Cl₂): λ_{\max} 344 nm. ¹H NMR (250 MHz, CDCl₃): δ 1.34 (d, $J_{\text{PH}} = 2.5$ Hz, Cp*, 15H), 2.16 (s, Me, 3H), 2.43 (s, Me, 3H), 3.32 (s, OMe, 3H), 6.31 (s, –CH, 1H), 6.42 (s, –CH, 1H), 6.5–7.5 (m, ArH, 13H). ³¹P{¹H} NMR (100 MHz, CDCl₃): δ 36.8 (d, $J_{\text{RHP}} = 162$ Hz), –143.8 (septet, $J_{\text{PF}} = 712$ Hz, PF₆[–]). FAB mass (m/z of cationic part): 777 (M⁺). Anal. Calc. for C₄₇H₄₇O₂P₂F₆Rh: C, 61.18; H, 5.13. Found C, 60.94; H, 5.05%.

Reaction of **1a** with 1-hexyne

A solution of **1a** (50 mg, 0.086 mmol), 1-hexyne (0.1 mL) and an excess of NaPF₆ in CH₂Cl₂-acetone (15 mL/10 mL) was stirred for 4 h. The solvent was evaporated and the residue was extracted with CH₂Cl₂. After the solution was concentrated to 3 mL, diethyl ether was added to give orange crystals of **6** (24 mg, 32%). IR (Nujol): 1660, 1593, 837 cm^{–1}. UV (CH₂Cl₂): λ_{\max} ca. 390 (sh), 283 nm. ¹H NMR (250 MHz, CDCl₃): δ 0.68 (t, $J_{\text{HH}} = 6.8$ Hz, CH₃, 3H), 1.03 (t, $J_{\text{HH}} = 6.8$ Hz, CH₃, 3H), 1.39 (d, $J_{\text{HH}} = 2.5$ Hz, Cp*, 15H), 1.2–2.8 (m, (CH₂)₃, 12H), 3.38 (s, OMe, 3H), 5.56 (s, CH=, 1H), 5.69 (d, $J_{\text{RHH}} = 15.0$ Hz, 1H), 6.6–7.8 (m, ArH, 13H). ³¹P{¹H} NMR (100 MHz, CDCl₃): δ 44.8 (d, $J_{\text{RHP}} = 157.5$ Hz), –143.8 (septet, $J_{\text{PF}} = 712$ Hz, PF₆[–]). Anal. Calc. for C₄₁H₅₁O₂P₂F₆Rh: C, 57.62; H, 6.01. Found C, 57.65; H, 5.85%.

Reaction of **1a** with 1-ethynyl-4-methoxycarbonylbenzene

A solution of **1a** (139 mg, 0.24 mmol), HC≡CC₆H₄COOMe-4 (107.4 mg, 0.67 mmol) and KPF₆ (144 mg, 0.78 mmol) in CH₂Cl₂ (5 mL) and acetone (20 mL) was stirred at room temperature. After 25 h, the solvent was removed and the residue was extracted with CH₂Cl₂ and a solution of CH₂Cl₂ was filtered with a glass filter (G4). The solvent was removed under reduced pressure. The residue was washed with diethyl ether and crystallized from CH₂Cl₂ and diethyl ether to give red crystals of **5c** (39 mg, 20%) and black brown crystals of **7** (57 mg, 24%). **5c**: IR (Nujol): 1717(C=O), 839 (P–F) cm^{–1}. UV (CH₂Cl₂): λ_{\max} 387, 290 (sh), 239 nm. ¹H NMR (250 MHz, CD₂Cl₂): δ 1.36 (d, $J_{\text{PH}} = 2.5$ Hz, Cp*, 15H), 3.35 (s, OMe, 3H), 3.88 (s, COOMe, 3H), 3.95 (s, COOMe, 3H), 6.49 (d, $J_{\text{HH}} = 8.5$ Hz, =CH, 1H), 8.19 (d, $J_{\text{HH}} = 8.5$ Hz, =CH, 1H), 6.5–7.7 (m, ArH, 21H). ³¹P{¹H} NMR (100 MHz, CD₂Cl₂): δ 35.8 (d, $J_{\text{RHP}} = 157.5$ Hz), –144.8 (sept, $J_{\text{PF}} = 712$ Hz). Anal. Calc. for C₄₉H₄₇O₆P₂F₆Rh: C, 58.22; H, 4.69. Found C, 58.14; H, 4.58%. **7**: IR (Nujol): 3285 (O–H), 1717 (C=O), 1605 (C=C), 839 (P–F) cm^{–1}. UV (CH₂Cl₂): λ_{\max} 404, 279 nm. ¹H NMR (250 MHz, CD₂Cl₂): δ 1.41 (d, $J_{\text{PH}} = 3.5$ Hz, Cp*, 15H), 3.44 (s, OMe, 3H), 3.83 (s, COOMe, 3H), 6.74 (s, OH, 1H), 5.8–8.0 (m, ArH, 17H). ³¹P{¹H} NMR (100 MHz, CD₂Cl₂): δ 29.7 (d, $J_{\text{RHP}} = 136.5$ Hz). Anal. Calc. for C₃₉H₄₀O₄PCl₂Rh·CH₂Cl₂: C, 55.71; H, 4.91. Found C, 55.10; H, 4.92%.

Reaction of **1a** with methylpropiolate

A solution of **1a** (110 mg, 0.189 mmol), HC≡CCOOMe (0.1 mL) and an excess of NaPF₆ in CH₂Cl₂ (5 mL) and acetone (10 mL) was stirred at room temperature. After 5 h, the solvent was removed under reduced pressure and the residue extracted with CH₂Cl₂. The solvent was removed. The residue was washed with diethyl ether and crystallized from CH₂Cl₂ and diethyl ether to give yellow orange crystals of **8a** (61 mg, 40%). IR (Nujol): 2060, 1699, 1583, 839 cm^{–1}. UV (CH₂Cl₂): λ_{\max} 293

nm. ¹H MNR (250 MHz, CDCl₃): δ 1.54 (d, $J_{\text{PH}} = 2.5$ Hz, Cp*, 15H), 3.16 (s, OMe, 3H), 3.76 (s, OMe, 3H), 6.7–7.8 (c, ArH, 13H), 7.96 (s, CH=, 1H). ³¹P{¹H} NMR (100 MHz, CDCl₃): δ 3.12 (d, $J_{\text{RHP}} = 122$ Hz), –143.9 Hz (septet, $J_{\text{PF}} = 712$ Hz, PF₆[–]). FAB mass (m/z of cation part): 658 (675.4). Anal. Calc. for C₃₄H₃₅O₅P₂F₆Rh: C, 51.14; H, 4.31. Found C, 50.89; H, 4.40%. Yellow complex **8b** (32%) was obtained from **1** with HC≡CCOOEt by a procedure similar to that for **8a**. IR (Nujol): 2060 (C=O), 1695 (C=O), 837 (PF₆) cm^{–1}. UV (CH₂Cl₂): λ_{\max} 310 nm. ¹H NMR (250 MHz, CDCl₃): δ 1.28 (t, $J_{\text{HH}} = 7.5$ Hz, Me, 3H), 1.54 (d, $J_{\text{PH}} = 2.5$ Hz, Cp*, 15H), 3.16 (s, OMe, 3H), 4.22 (q, $J_{\text{HH}} = 7.5$ Hz, OCH₂, 2H), 6.7–7.8 (m, ArH, 13H), 7.96 (s, CH=, 1H). ³¹P{¹H} NMR (100 MHz, CDCl₃): δ 3.15 (d, $J_{\text{RHP}} = 125$ Hz), –143.9 (septet, $J_{\text{PF}} = 711.0$ Hz, PF₆[–]). Anal. Calc. for C₃₅H₃₇O₅P₂F₆Rh: C, 51.80; H, 4.51. Found C, 51.48; H, 4.57%.

Reaction of **1a** with EtOOC≡CCOOEt

Reddish orange crystals **9b** (45 mg, 63%) were obtained from **1a** (55 mg, 0.095 mmol), EtOOC≡CCOOEt (0.1 mL) and an excess of NaPF₆ by a procedure similar to that for **8a**. IR (Nujol): 1705 (C=O), 1589 (C=C) cm^{–1}. UV (CH₂Cl₂): λ_{\max} ca. 400(sh), 328 nm. ¹H NMR (250 MHz, CDCl₃): δ 1.03 (t, $J_{\text{HH}} = 7.0$ Hz, Me, 3H), 1.27 (t, $J_{\text{HH}} = 7.0$ Hz, Me, 3H), 1.26 (d, $J_{\text{PH}} = 3.0$ Hz, Cp*, 15H), 3.03 (s, OMe, 3H), 4.03 (m, CH₂, 2H), 4.18 (m, CH₂, 2H), 7.0–7.9 (m, Ph, 13H). ³¹P{¹H} NMR (100 MHz, CDCl₃): δ 10.3 (d, $J_{\text{RHP}} = 137$ Hz, 1P). FAB mass (m/z of cation part): 737 ([M – CO]⁺). Anal. Calc. for C₃₇H₄₁O₆PClRh·0.5CH₂Cl₂: C, 56.76; H, 5.34. Found C, 56.56; H, 5.22%. **9a** (57%) was obtained from the reaction between **1a** (30 mg, 0.052 mmol), MeOOC≡CCOOMe (0.15 mL) and NaPF₆ (24 mg, 0.14 mmol). IR (Nujol): 1705 (C=O), 1581 (C=C) cm^{–1}. UV (CH₂Cl₂): λ_{\max} 364, 266 nm. ¹H NMR (250 MHz, CDCl₃): δ 1.25 (d, $J_{\text{PH}} = 3.0$ Hz, Cp*, 15H), 3.04 (s, OMe, 3H), 3.53 (s, OMe, 3H), 3.74 (s, OMe, 3H), 5.28 (s, CH₂Cl₂, 2H), 6.6–7.7 (m, Ph, 13H). ³¹P{¹H} NMR (100 MHz, CDCl₃): δ 10.3 (d, $J_{\text{RHP}} = 137.5$ Hz, 1P). FAB mass (m/z of cation part): 709 ([M – CO]⁺). Anal. Calc. for C₃₅H₃₇O₆PClRh·0.5CH₂Cl₂: C, 55.70; H, 5.00. Found C, 55.20; H, 4.75%.

Reaction of **2a** with 1-ethynyl-4-methoxycarbonylbenzene

A solution of **2a** (45.7 mg, 0.071 mmol), HC≡CC₆H₄COOMe-4 (37.6 mg, 0.235 mmol) and KPF₆ (37.2 mg, 0.202 mmol) in CH₂Cl₂ (5 mL) and acetone (20 mL) was stirred at room temperature. After 8 h, the solvent was removed and the residue was extracted with CH₂Cl₂ and a solution of CH₂Cl₂ was filtered with a glass filter (G4). The solvent was removed under reduced pressure. The residue was washed with diethyl ether and crystallized from CH₂Cl₂ and diethyl ether to give yellow solid **10a** (27.8 mg, 43%). IR (Nujol): 1715 (C=O), 1630 (C=O) and 839 (P–F) cm^{–1}. UV (CH₂Cl₂): λ_{\max} 405, 284 nm. ¹H NMR (250 MHz, CDCl₃): δ 1.74 (d, $J_{\text{PH}} = 3.5$ Hz, Cp*, 15H), 2.97 (s, OMe, 3H), 3.06 (bs, OMe, 6H), 3.48 (bs, OMe, 3H), 3.84 (s, COOMe, 3H), 5.59 (d, $J_{\text{RHH}} = 7.0$ Hz, CH=, 1H) 5.6–7.2 (m, ArH, 15H). ³¹P{¹H} NMR (100 MHz, CDCl₃): δ 138.7 (d, $J_{\text{RHP}} = 153$ Hz), –143.7 (septet, $J_{\text{PF}} = 712$ Hz, PF₆[–]). FAB mass (m/z of cation part): 765 ([M – 1]⁺), 605 ([M – (HC=C₆H₅COOMe)]⁺). Anal. Calc. for C₄₁H₄₃O₆P₂F₆Rh: C, 54.08; H, 4.76. Found C, 53.82; H, 4.81%. Brown complex **10b** (18%) was obtained from the reaction of **2a** and HC≡CC₆H₄NO₂-4. IR (Nujol): 1628 (C=O), 835 (PF₆) cm^{–1}. ¹H NMR (CD₂Cl₂): δ 1.74 (d, $J_{\text{PH}} = 3.5$ Hz, Cp*, 15H), 2.99 (s, MeO, 3H), 3.08 (br, MeO, 3H), 3.52 (br, MeO, 3H), 5.68 (d, $J_{\text{RHH}} = 7.5$ Hz, CH=, 1H), 6.4–8.2 (m, Ph and ring Protons). ³¹P{¹H} NMR (CDCl₃): δ 140.4 (d, $J_{\text{RHH}} = 153$ Hz), –143.7 (septet, $J_{\text{PF}} = 712$ Hz, PF₆[–]). FAB mass (m/z of cation part): 752 ([M – PF₆]⁺), 605 ([M – PF₆ – HC≡CC₆H₄NO₂]⁺). Anal. Calc. for C₃₉H₄₀NO₆P₂F₆Rh·CH₂Cl₂: C, 48.90; H, 4.31; N, 1.43. Found C, 49.19; H, 4.40; N, 1.52%.

Reaction of **2a** with methylpropiolate

Yellow crystals of **11a** were prepared by the reaction of **2a** (40.8 mg, 0.064 mmol), KPF₆ (39.0 mg, 0.212 mmol) and HC≡CCOOMe (0.05 mL, 0.60 mmol) at room temperature for 9 h, according to a procedure similar to that for **8a**. IR (Nujol): 2064, 1694, 841 cm⁻¹. UV (CH₂Cl₂): λ_{max} 298 nm. ¹H NMR (250 MHz, CDCl₃): δ 1.62 (d, J_{PH} = 3.8 Hz, Cp*, 15H), 3.24 (s, OMe, 3H), 3.31 (s, OMe, 3H), 3.68 (s, OMe, 3H), 3.85 (s, COOMe, 3H), 6.5–7.7 (m, ArH, 11H), 7.92 (s, CH=, 1H). ³¹P{¹H} NMR (100 MHz, CDCl₃): δ -13.4 (d, J_{RHP} = 126.5 Hz), -143.8 (septet, J_{PF} = 712 Hz, PF₆⁻). FAB mass (*m/z* of cation part): 717 ([M - I]⁺), 689 ([M - CO]⁺), 605 (M - CO - (CH=CCOOMe))⁺. Anal. Calc. for C₃₆H₃₉O₇P₂F₆Rh: C, 50.13; H, 4.56. Found C, 49.89; H, 4.41%.

Brown complex **11b** (15 mg, 33%) was obtained by the reaction of **2a** (33.2 mg, 0.052 mmol), KPF₆ (29.4 mg, 0.160 mmol) and HC≡CCOOEt (0.05 mL, 0.489 mmol) at room temperature for 4 h, according to a procedure similar to that for **8a**. IR (Nujol): 2062 (CO), 1688 (C=O), 841 cm⁻¹. UV (CH₂Cl₂): λ_{max} 298, 232 nm. ¹H NMR (250 MHz, CDCl₃): δ 1.33 (t, J_{HH} = 7.0 Hz, Me, 3H), 1.59 (d, J_{PH} = 4.0 Hz, Cp*, 15H), 3.22 (s, OMe, 3H), 3.28 (s, OMe, 3H), 3.64 (s, OMe, 3H), 4.28 (q, J_{HH} = 7.0 Hz, CH₂, 2H), 6.5–7.7 (c, ArH, 11H), 7.90 (s, CH=, 1H). ³¹P{¹H} NMR (100 MHz, CDCl₃): δ -13.5 (d, J_{RHP}, 132 Hz), -143.8 Hz (septet, J_{PF} = 712 Hz, PF₆⁻). FAB mass (*m/z* of cation part): 731 ([M - I]⁺), 703 ([M - CO + I]⁺), 605 (M - CO - (CH=CCOOEt))⁺. Anal. Calc. for C₃₇H₄₁O₇P₂F₆Rh: C, 50.70; H, 4.71. Found C, 50.92; H, 4.55%.

Reaction of **2a** with MeOOC≡CCOOMe

Reddish orange crystals **12a** (47.3 mg, 56%) were obtained from **2** (69.6 mg, 0.109 mmol), MeOOC≡CCOOMe (0.2 mL, 1.63 mmol) and KPF₆ (61.2 mg, 0.333 mmol) at room temperature for 5 h by a procedure similar to that for **9b**. IR (Nujol): 1707 (C=O) cm⁻¹. UV (CH₂Cl₂): λ_{max} 371, 274 nm. ¹H NMR (250 MHz, CDCl₃): δ 1.34 (d, J_{PH} = 3.0 Hz, Cp*, 15H), 3.07 (s, OMe, 3H), 3.23 (s, OMe, 3H), 3.58 (s, OMe, 3H), 3.77 (s, COOMe, 3H), 6.3–7.6 (m, Ph, 13H). ³¹P{¹H} NMR (100 MHz, CDCl₃): δ -1.92 (d, J_{RHP} = 151.5 Hz, 1P). FAB mass (*m/z*): 782 ([M - I]⁺), 747 ([M - Cl - I]⁺), 605 ([M - Cl - (MeOOC≡CCOOMe)]⁺). Anal. Calc. for C₃₇H₄₁O₈PClRh: C, 56.75; H, 5.28. Found C, 56.35; H, 5.34%. Complex **12b** (45.3 mg, 47%) was prepared by the reaction of **2a** (76.5 mg, 0.119 mmol), MeOOC≡CCOOMe (0.2 mL, 1.26 mmol) and KPF₆ (60.5 mg, 0.329 mmol) at room temperature for 44 h by a procedure similar to that for **9b**. IR (Nujol): 1703 (C=O) cm⁻¹. UV (CH₂Cl₂): λ_{max} 371, 273 nm. ¹H NMR (250 MHz, CDCl₃): δ 1.34 (d, J_{PH} = 3.0 Hz, Cp*, 15H), 3.07 (s, OMe, 3H), 3.22 (s, OMe), 3.58 (s, OMe), 4.18–4.27 (m, COOCH₂Me, 2H), 6.3–7.6 (m, Ph, 13H). ³¹P{¹H} NMR (100 MHz, CDCl₃): δ -2.02 (d, J_{RHP} = 151.0 Hz, 1P). FAB mass (*m/z*): 811 ([M]⁺), 641 ([M - (EtOOC≡CCOOEt)]⁺), 605 ([M - Cl - (EtOOC≡CCOOEt)]⁺). Anal. Calc. for C₃₉H₄₅O₈PClRh: C, 57.75; H, 5.59. Found C, 57.41; H, 5.59%.

Reaction of **1b** with ethynylbenzene

To a solution of **1b** (122 mg, 0.182 mmol) and PHC≡CH (0.25 mL, 2.28 mmol) in CH₂Cl₂ (5 mL) and MeOH (20 mL) was added KPF₆ (151.2 mg, 0.82 mmol) at room temperature. After 24 h, the solvent was removed and the residue extracted with CH₂Cl₂. The solvent was removed under reduced pressure and the residue was recrystallized from CH₂Cl₂ and diethyl ether to give pale yellow crystals of **14** (25.2 mg, 17%). The solvent was removed from the mother-liquor and the residue was recrystallized from CH₂Cl₂ and diethyl ether to give yellow crystals of **13a** (45 mg, 27%) **13a**: IR (Nujol): 837 cm⁻¹. UV (CH₂Cl₂): λ_{max} 322, 232 nm. ¹H NMR (250 MHz, CDCl₃): δ 1.46 (d, J_{PH} = 2.0 Hz, Cp*, 15H), 3.37 (s, OMe, 3H), 3.83 (s, =COMe, 3H),

4.13 (s, CH₂, 1H) 4.18 (s, CH₂, 1H), 6.0–7.7 (m, ArH, 18H). ³¹P{¹H} NMR (100 MHz, CDCl₃): δ 19.1 (s), -143.7 (septet, J_{PF} = 712 Hz, PF₆⁻). Anal. Calc. for C₃₈H₄₁O₃P₂F₆Ir: C, 49.94; H, 4.52. Found C, 49.68; H, 4.51%.

Complex **13b** together with a small amount of **14** was obtained from the reaction between **1b** and the corresponding 1-alkyne in the presence of KPF₆, according to a procedure similar to that of **13a**. **13b**: IR (Nujol): 837 cm⁻¹. UV (CH₂Cl₂): λ_{max} 328 nm. ¹H NMR (250 MHz, CD₂Cl₂): δ 1.48 (d, J_{PH} = 2.0 Hz, Cp*, 15H), 2.31 (s, Me, 3H), 3.38 (s, OMe, 3H), 3.75 (s, =COMe, 3H), 4.15 (s, CH₂, 1H), 4.21 (s, CH₂, 1H), 6.1–7.8 (m, ArH, 18H). ³¹P{¹H} NMR (100 MHz, CDCl₃): δ 18.8 (s), -144.7 (septet, J_{PF} = 712 Hz, PF₆⁻).

Reaction of **1b** with 1-ethynyl-4-methoxycarbonylbenzene

A solution of **1b** (144.8 mg, 0.216 mmol), HC≡CC₆H₄COOMe-4 (72.9 mg, 0.455 mmol) and KPF₆ (105.3 mg, 0.572 mmol) in CH₂Cl₂ (5 mL) and acetone (20 mL) was stirred at room temperature. After 24 h, the solvent was removed and the residue extracted with CH₂Cl₂ and a solution of CH₂Cl₂ was filtered with a glass filter. The solvent was removed under reduced pressure. The residue was washed with diethyl ether and crystallized from CH₂Cl₂ and diethyl ether to give orange crystals of **16** (25 mg, 14%). Work-up of the mother-liquor and recrystallization from CH₂Cl₂ and diethyl ether gave orange crystals of **15** (67 mg, 28%). **15**: IR (Nujol): 3312 (OH), 1717 (C=O) cm⁻¹. UV (CH₂Cl₂): λ_{max} 271 nm. ¹H NMR (250 MHz, CD₂Cl₂): δ 1.44 (d, J_{PH} = 2.0 Hz, Cp*, 15H), 3.45 (s, OMe, 3H), 3.84 (s, COOMe, 3H), 6.64 (s, OH, 1H), 5.8–8.0 (m, ArH, 17H). ³¹P{¹H} NMR (100 MHz, CD₂Cl₂): δ 3.54 (s). Anal. Calc. for C₃₉H₄₀O₄PCl₂Ir·CH₂Cl₂: C, 50.48; H, 4.65. Found C, 50.38; H, 4.53%. **16**: IR (Nujol): 1721(C=O), 843 (P-F) cm⁻¹. UV (CH₂Cl₂): λ_{max} 325(sh), 270(sh) nm. ¹H NMR (250 MHz, CD₂Cl₂): δ 1.29 (d, J_{PH} = 2.0 Hz, Cp*, 15H), 3.67 (s, OMe, 3H), 3.89 (s, COOMe, 3H), 3.90 (s, COOMe, 3H), 5.2–7.9 (m, CH= and ArH, 21H). ³¹P{¹H} NMR (100 MHz, CD₂Cl₂): δ 21.9 (s), -143.8 (septet, J_{PF} = 712 Hz, PF₆⁻). FAB mass (*m/z*): 955 ([M]⁺), 794 ([M - (CH=CC₆H₄COOMe) - I]⁺), 635 ([M - (CH=CC₆H₄COOMe)₂]⁺). Anal. Calc. for C₄₉H₄₇O₆P₂F₆Ir: C, 53.50; H, 4.31. Found C, 53.14; H, 4.48%.

Reaction of **1b** with MeOOC≡CCOOMe

Yellow crystals of **17a** (34.7 mg, 44%) were obtained from **1b** (65.3 mg, 0.097 mmol), MeOOC≡CCOOMe (0.15 mL, 1.22 mmol) and KPF₆ (72 mg, 0.391 mmol) by a procedure similar to that for **8a**. IR (Nujol): 1703 (C=O). UV (CH₂Cl₂): λ_{max} 294(sh) nm. ¹H NMR (250 MHz, CDCl₃): δ 1.28 (d, J_{PH} = 2.0 Hz, Cp*, 15H), 3.03 (s, OMe, 3H), 3.62 (s, COOMe, 3H), 3.76 (s, COOMe, 3H), 6.6–7.7 (m, Ph, 13H). ³¹P{¹H} NMR (100 MHz, CDCl₃): δ -23.8 (s). Anal. Calc. for C₃₅H₃₇O₆PClIr: C, 51.75; H, 4.59. Found C, 50.35; H, 4.62%.

Analogously, complexes **17b**, **18a** and **18b** were prepared from the corresponding compounds, according to a procedure similar to that for **8a**. **17b**: IR (Nujol): 1698 (C=O) cm⁻¹. UV (CH₂Cl₂): λ_{max} 291(sh) nm. ¹H NMR (250 MHz, CDCl₃): δ 1.12 (t, J_{HH} = 7.0 Hz, Me, 3H), 1.28 (d, J_{PH} = 2.0 Hz, Cp*, 15H), 1.30 (t, J_{HH} = 7.0 Hz, Me, 3H), 3.03 (s, OMe, 3H), 4.0–4.25 (m, CH₂, 4H), 6.5–7.7 (m, Ph, 13H). ³¹P{¹H} NMR (100 MHz, CDCl₃): δ -24.0 (s). Anal. Calc. for C₃₇H₄₁O₆PClIr: C, 52.88; H, 4.92. Found C, 52.99; H, 5.20%. **18a** (yellow, 68%) IR (Nujol): 1709 (C=O) cm⁻¹. UV (CH₂Cl₂): λ_{max} 288 nm. ¹H NMR (250 MHz, CDCl₃): δ 1.31 (d, J_{PH} = 2.0 Hz, Cp*, 15H), 3.02 (s, OMe, 3H), 3.20 (s, OMe, 3H), 3.56 (s, OMe, 3H), 3.75 (s, COOMe, 3H), 3.77 (s, COOMe, 3H), 6.3–7.7 (m, Ph, 11H). ³¹P{¹H} NMR (100 MHz, CDCl₃): δ -36.4 (s). FAB mass (*m/z* of cation part): 872 ([M]⁺), 837 ([M - Cl]⁺), 695 ([M - Cl - MeOOC≡CCOOMe]⁺). Anal. Calc. for C₃₇H₄₁O₈PClIr: C, 50.94; H, 4.74. Found C, 50.97; H, 4.74%. **18b** (yellow, 28%): IR (Nujol): 1709, 1694 (C=O) cm⁻¹. ¹H NMR (250 MHz, CDCl₃): δ 1.32 (t,

$J_{\text{HH}} = 7.0$ Hz, Me, 3H), 1.34 (d, $J_{\text{PH}} = 2.0$ Hz, Cp*, 15H), 1.35 (d, $J_{\text{HH}} = 7.0$ Hz, Me, 3H), 3.04 (s, OMe, 3H), 3.22 (s, OMe, 3H), 3.58 (s, OMe, 3H) 4.15–4.33 (m, CH₂, 4H), 6.5–7.7 (m, Ph, 11H). ³¹P{¹H} NMR (100 MHz, CDCl₃): δ -36.2 (s). Anal. Calc. for C₃₉H₄₅O₈PClIr: C, 52.02; H, 5.04. Found C, 52.36; H, 5.20%.

Reactions of **9** with Lewis bases

(a) **With xylyl isocyanide in the presence of KPF₆**. A solution of **9a** (74.7 mg, 0.103 mmol), xylyl isocyanide (45 mg, 0.343 mmol) and KPF₆ (64.8 mg, 0.352 mmol) in CH₂Cl₂ (25 mL) and acetone (20 mL) was stirred at room temperature for 24 h. After the solvent was removed under reduced pressure, the residue was extracted with CH₂Cl₂. After CH₂Cl₂ was removed, the residue was washed with diethyl ether and recrystallized from CH₂Cl₂ and diethyl ether to give yellow crystals of **19ace** (87.3 mg, 88%). IR (Nujol): 2159 (N≡C), 1734 (C=O), 837 (P–F) cm⁻¹. UV (CH₂Cl₂): λ_{max} 313(sh), 235 nm. ¹H NMR (250 MHz, CDCl₃): δ 1.51 (d, $J_{\text{PH}} = 3.5$ Hz, Cp*, 15H), 2.01 (s, *o*-Me, 6H), 3.22 (s, OMe, 3H), 3.79 (s, COOMe, 3H), 3.83 (s, COOMe, 3H), 6.6–7.9 (m, Ph, 13H). ³¹P{¹H} NMR (100 MHz, CDCl₃): δ 7.16 (s), -143.8 (septet, $J_{\text{PF}} = 712$ Hz, PF₆⁻). Anal. Calc. for C₄₄H₄₆NO₆F₆P₂Rh: C, 54.84; H, 4.81; N, 1.45. Found C, 54.64; H, 4.79; N, 1.54%.

(b) **With xylyl isocyanide or mesityl isocyanide in the presence of Ag(OTf)**. A solution of **9a** (146.4 mg, 0.203 mmol), xylyl isocyanide (55.5 mg, 0.423 mmol) and Ag(OTf) (52.6 mg, 0.205 mmol) in CH₂Cl₂ (5 mL) and acetone (15 mL) was stirred at room temperature for 24 h. The work-up similar to that for **19ace** gave yellow crystals of **19acf** (55.8 mg, 28%). IR (Nujol): 2159 (N≡C), 1717 (C=O), 1209 (OTf), 1030 (OTf), 635 (OTf) cm⁻¹. UV (CH₂Cl₂): λ_{max} 314(sh), 235 nm. ¹H NMR (250 MHz, CDCl₃): δ 1.51 (d, $J_{\text{PH}} = 3.5$ Hz, Cp*, 15H), 2.09 (s, *o*-Me, 6H), 3.22 (s, OMe, 3H), 3.78 (s, COOMe, 3H), 3.81 (s, COOMe, 3H), 6.6–7.8 (m, Ph, 16H). ³¹P{¹H} NMR (100 MHz, CDCl₃): δ 6.4 (d, $J_{\text{RHP}} = 127$ Hz). Anal. Calc. for C₄₄H₄₆NO₉F₃PSRh: C, 55.85; H, 4.79; N, 1.45. Found C, 55.74; H, 4.82; N, 1.54%. **19adf** (yellow, 57%): a procedure similar to that for **19ace** was carried out except the reaction time of 5 h. IR (Nujol): 2153 (N≡C), 1719 (C=O), 1703 (C=O), 1032 (OTf), 637 (OTf) cm⁻¹. UV (CH₂Cl₂): λ_{max} 312 (sh), 245 nm. ¹H NMR (250 MHz, CD₂Cl₂): δ 1.50 (d, $J_{\text{PH}} = 3.5$ Hz, Cp*, 15H), 2.04 (s, *o*-Me, 6H), 2.29 (s, *p*-Me, 3H), 3.22 (s, OMe, 3H), 3.78 (s, COOMe, 3H), 3.80 (s, COOMe, 3H), 6.7–7.9 (m, Ph, 15H). ³¹P{¹H} NMR (100 MHz, CD₂Cl₂): δ 6.45 (d, $J_{\text{RHP}} = 127.5$ Hz). Anal. Calc. for C₄₆H₄₈NO₉F₃PSRh: C, 56.27; H, 4.93; N, 1.43. Found C, 56.30; H, 5.46; N, 1.36%. **19bcf** (yellow, 85%): A procedure similar to that for **19ace** was carried out except the reaction time of 5 h. IR (Nujol): 2153 (N≡C), 1725 (C=O), 1705 (C=O), 1032 (OTf), 637 (OTf) cm⁻¹. UV (CH₂Cl₂): λ_{max} 312 (sh), 235 nm. ¹H NMR (250 MHz, CD₂Cl₂): δ 1.26 (t, $J_{\text{HH}} = 7.0$ Hz, Me, 3H), 1.33 (t, $J_{\text{HH}} = 7.0$ Hz, Me, 3H), 1.53 (d, $J_{\text{PH}} = 3.5$ Hz, Cp*, 15H), 2.05 (s, *o*-Me, 6H), 3.22 (s, OMe, 3H), 4.23 (q, CH₂, $J_{\text{HH}} = 7.0$ Hz, 4H), 6.6–7.9 (m, Ph, 16H). ³¹P{¹H} NMR (100 MHz, CD₂Cl₂): δ 7.16 (d, $J_{\text{RHP}} = 127$ Hz). Anal. Calc. for C₄₇H₅₀NO₉F₃PSRh: C, 56.69; H, 5.06; N, 1.41. Found C, 56.41; H, 5.06; N, 1.49%. **19bdf** (yellow, 38%): A procedure similar to that for **19ace** was carried out except the reaction time of 5 h. IR (Nujol): 2151 (N≡C), 1717 (C=O), 1696 (C=O), 1034 (OTf), 637 (OTf) cm⁻¹. UV (CH₂Cl₂): λ_{max} 315 (sh), 238 nm. ¹H NMR (250 MHz, CDCl₃): δ 1.26 (t, $J_{\text{HH}} = 7.0$ Hz, Me, 3H), 1.33 (t, $J_{\text{HH}} = 7.0$ Hz, Me, 3H), 1.52 (d, $J_{\text{PH}} = 3.5$ Hz, Cp*, 15H), 2.00 (s, *o*-Me, 6H), 2.28 (s, *p*-Me, 3H), 3.23 (s, OMe, 3H), 4.23 (q, $J_{\text{HH}} = 7.0$ Hz, CH₂, 4H), 6.6–7.9 (m, Ph, 15H). ³¹P{¹H} NMR (100 MHz, CDCl₃): δ 7.21 (d, $J_{\text{RHP}} = 127$ Hz). Anal. Calc. for C₄₈H₅₂NO₉F₃PSRh: C, 52.45; H, 4.77; N, 1.27. Found C, 52.41; H, 5.00; N, 1.37%.

(c) **With carbon monoxide in the presence of Ag(OTf)**. Carbon monoxide was bubbled into a solution of **9a** (153.3 mg,

0.212 mmol) and Ag(OTf) (202.7 mg, 0.789 mmol) in CH₂Cl₂ (25 mL) and acetone (25 mL) at room temperature for 3 min. After 5 h, work-up similar to that for **19ace** gave yellow solid **20a** (158.2 mg, 69%). IR (Nujol): 2068 (C≡O), 1715 (C=O), 1028, 637, 573 (OTf) cm⁻¹. UV (CH₂Cl₂): λ_{max} 303(sh), 235 nm. ¹H NMR (250 MHz, CDCl₃): δ 1.60 (d, $J_{\text{PH}} = 4.0$ Hz, Cp*, 15H), 3.18 (s, OMe, 3H), 3.75 (s, COOMe, 3H), 3.82 (s, COOMe, 3H), 6.7–7.8 (m, Ph, 13H). ³¹P{¹H} NMR (100 MHz, CDCl₃): δ 3.31 (d, $J_{\text{RHP}} = 122$ Hz).

Preparation of **21**

(a) **With 1a and MeOOC≡CCOOMe in the presence of Ag(OTf)**. A solution of **1a** (143.6 mg, 0.25 mmol), MeOOC≡CCOOMe (0.25 mL, 2.04 mmol) and Ag(OTf) (131.4 mg, 0.511 mmol) in MeOH (20 mL) and CH₂Cl₂ (5 mL) was stirred for 7 h at room temperature. The solvent was removed under reduced pressure. The oily product was chromatographed on alumina (contained 10% H₂O) using ethyl acetate as an eluent. The eluting solution was concentrated and the residue recrystallized from CH₂Cl₂ and diethyl ether to give orange crystals **21** (63.2 mg, 26%). IR (Nujol): 1732, 1709 (C=O), 841 (P–F) cm⁻¹. UV (CH₂Cl₂): λ_{max} 288(sh), 236 nm. ¹H NMR (250 MHz, CDCl₃): δ 1.48 (d, $J_{\text{PH}} = 3.0$ Hz, Cp*, 15H), 2.79 (s, OMe, 3H), 3.44 (s, COOMe, 3H), 3.55 (s, COOMe, 3H), 3.92 (s, COOMe, 3H), 4.05 (s, COOMe, 3H), 6.7–7.7 (m, Ph, 13H). ³¹P{¹H} NMR (100 MHz, CDCl₃): δ -35.3 (d, $J_{\text{RHP}} = 148$ Hz). FAB mass (m/z of cationic part): 828 ([M - 1]⁺), 545 ([M - (MeOOC≡CCOOMe)₂]⁺). Anal. Calc. for C₄₂H₄₃O₁₃F₃PSRh: C, 49.96; H, 4.29. Found C, 50.00; H, 4.39%.

(2) **With 9a and MeOOC≡CCOOMe in the presence of Ag(OTf)**. Complex **21** was generated from **9a** and MeOOC≡CCOOMe in the presence of Ag(OTf) according to a procedure similar to (a).

Reaction of [Cp*Ir(CO)(MDMPP-*P*,*O*)](PF₆) **14** with MeOOC≡CCOOMe

(a) **In MeOH**. A solution of **14** (138 mg, 0.17 mmol) and MeOOC≡CCOOMe (0.25 mL, 2.04 mmol) in MeOH (40 mL) was refluxed for 20 h. The solvent was removed under reduced pressure. The residue was washed with diethyl ether and crystallized from CH₂Cl₂ and diethyl ether to give [Cp*Ir(CO)(PPh₂(C₆H₃-2-(MeO)-6-(OC(COOMe)=C(COOMe)))](PF₆) **22** (86.6 mg, 44%). IR (Nujol): 2066 (C≡O), 1717 (C=O), 841 (P–F) cm⁻¹. UV (CH₂Cl₂): λ_{max} 298(sh), 269(sh) nm. ¹H NMR (250 MHz, CDCl₃): δ 1.65 (d, $J_{\text{PH}} = 2.5$ Hz, Cp*, 15H), 3.16 (s, OMe, 3H), 3.76 (s, COOMe, 3H), 3.82 (s, COOMe, 3H), 6.7–7.8 (m, Ph, 13H). ³¹P{¹H} NMR (100 MHz, CDCl₃): δ -36.6 (s), -143.9 (septet, $J_{\text{PF}} = 172$ Hz, PF₆⁻). FAB mass (m/z of cationic part): 804 ([M]⁺), 775 ([M - CO + 2]⁺), 635 ([M - CO - (MeOOC≡CCOOMe)]⁺). Anal. Calc. for C₃₈H₄₁O₈F₆P₂Ir: C, 45.92; H, 4.16. Found C, 45.88; H, 4.09%.

(b) **In CH₂Cl₂**. Complex **17a** (38%) was obtained from [Cp*Ir(CO)(MDMPP-*P*,*O*)](PF₆) **14** and MeOOC≡CCOOMe in CH₂Cl₂ at reflux for 8 h.

(c) **In MeOH and CH₂Cl₂**. Complexes **17a** (23%) and **22** (17%) were obtained from **14** (69.0 mg, 0.09 mmol) and MeOOC≡CCOOMe (0.13 mL, 1.02 mmol) in MeOH (15 mL) and CH₂Cl₂ (15 mL) at reflux for 10 h.

Data collection

All complexes were recrystallized from acetone–diethyl ether or CH₂Cl₂–diethyl ether. Cell constants were determined from 20–25 reflections on a Rigaku four-circle automated diffractometer AFC5S. The crystal parameters along with data collections are summarized in Table 9. Data collections were carried out on

Table 9 Crystal data for [Cp*RhCl(BDMPP-*P*,*O*)] **2a**, [Cp*Rh(TDMPP-*P*,*O*,*O'*)] **4a**, [Cp*Rh{PPh₂(C₆H₃-2-(MeO)-6-(OC(Tol)=CHCH=C(Tol)))](PF₆) **5b**, [Cp*Rh{PPh₂(C₆H₃-2-(MeO)-6-(OC(C₆H₄-4-COOMe)=CHCH=C(C₆H₄-4-COOMe)))](PF₆) **5c**, [Cp*Rh{PPh₂(C₆H₃-2-(MeO)-6-(OC(*n*Bu)CH=CC(*n*Bu)=CH)))](PF₆) **6**, [Cp*Rh(CO){PPh₂(C₆H₃-2-(MeO)-6-(OCH=C(COOMe)))](PF₆) **8a**, [Cp*Rh(BDMPP-*P*,*O*)-(HC≡CC₆H₄NO₂)] (PF₆) **10b**·3H₂O, [Cp*Rh(CO){PPh(C₆H₃-2,6-(MeO)₂)(C₆H₃-2-(MeO)-6-(O-CH=C(COOMe)))](PF₆) **11a**, [Cp*RhCl{PPh(C₆H₃-2,6-(MeO)₂)(C₆H₃-2-(MeO)-6-(OC(COOR)=C(COOR)))] **12b**, [Cp*Ir(MDMPP-*P*,*O*){=C(OMe)CH₂R}](PF₆) **13a**, [Cp*IrCl{PPh(C₆H₃-2,6-(MeO)₂)(C₆H₃-2-(MeO)-6-(OC(COOMe)=C(COOMe)))] **18a**, [Cp*IrCl{PPh(C₆H₃-2,6-(MeO)₂)(C₆H₃-2-(MeO)-6-(OC(COOEt)=C(COOEt)))] **18b** and [Cp*Rh{PPh₂(C₆H₃-2-(MeO)-6-(OC(COOEt)=C(COOEt)))](CNXyl)(PF₆) **19bcf**

Compound	2a	4a	5b	5c	6	8a	10b ·3H ₂ O	11a	12b	13a	18a	18b	19bcf
Formula	C ₃₁ H ₃₅ O ₄ -PClRh	C ₃₂ H ₃₆ O ₆ PRh	C ₄₇ H ₄₇ O ₂ -P ₂ F ₆ Rh	C ₄₉ H ₄₇ O ₆ -P ₂ F ₆ Rh	C ₄₁ H ₅₁ O ₂ -P ₂ F ₆ Rh	C ₃₄ H ₃₅ O ₅ -P ₂ F ₆ Rh	C ₃₉ H ₄₆ NO ₉ -P ₂ F ₆ Rh	C ₃₆ H ₃₉ O ₇ -P ₂ F ₆ Rh	C ₃₉ H ₄₅ O ₈ -PClRh	C ₃₈ H ₄₁ O ₃ -P ₂ F ₆ Ir	C ₃₇ H ₄₁ O ₈ -PClIr	C ₃₉ H ₄₅ O ₈ -PClIr	C ₄₇ H ₅₀ NO ₉ -PF ₃ SRh
Mol. wt	640.95	650.51	922.73	1010.75	854.7	802.49	951.64	862.54	811.11	913.3	862.54	900.43	995.85
Crystal system	Monoclinic	Orthorhombic	Monoclinic	Monoclinic	Triclinic	Monoclinic	Monoclinic	Monoclinic	Monoclinic	Monoclinic	Monoclinic	Monoclinic	Monoclinic
Space group	<i>P2₁/n</i> (no. 14)	<i>Pbcn</i> (no. 60)	<i>P2₁/a</i> (no. 14)	<i>P2₁/a</i> (no. 14)	<i>P1</i> (no. 2)	<i>P2₁/a</i> (no. 14)	<i>P2₁/c</i> (no. 14)	<i>P2₁/c</i> (no. 14)	<i>P2₁/n</i> (no. 14)	<i>P2₁/n</i> (no. 14)	<i>P2₁/n</i> (no. 14)	<i>P2₁/c</i> (no. 14)	<i>P2₁/o</i> (no. 14)
<i>a</i> /Å	16.018(7)	17.507(6)	15.74(1)	15.534(3)	11.575(4)	15.411(3)	15.299(7)	10.797(7)	12.031(7)	15.060(9)	11.049(3)	12.515(8)	11.146(4)
<i>b</i> /Å	10.46(1)	21.180(7)	17.42(1)	19.986(3)	16.67(1)	22.199(4)	14.826(7)	24.881(8)	17.48(1)	13.360(8)	16.085(3)	12.00(2)	14.634(3)
<i>c</i> /Å	17.695(4)	15.903(8)	16.32(1)	15.757(3)	10.800(5)	10.602(4)	19.505(9)	14.146(6)	18.152(4)	18.705(9)	19.689(4)	25.04(2)	28.41(2)
<i>α</i> ^o	90.0	90.0	90.0	90.0	90.17(5)	90.0	90.0	90.0	90.0	90.0	90.0	90.0	90.0
<i>β</i> ^o	94.06(3)	90.0	102.66(6)	103.70(1)	99.46(3)	110.11(3)	106.78(3)	96.16(4)	99.39(3)	90.84(4)	96.17(2)	95.29(8)	91.75(4)
<i>γ</i> ^o	90.0	90.0	90.0	90.0	93.41(4)	90.0	90.0	90.0	90.0	90.0	90.0	90.0	90.0
<i>V</i> /Å ³	2957(3)	5896(3)	4364(5)	4752(1)	2051(1)	3405(1)	4235(3)	3778(2)	3766(3)	3763(3)	3478(1)	3834(6)	4631(3)
<i>Z</i>	5	8	4	4	2	4	4	4	4	4	4	4	4
<i>D_c</i> /g cm ⁻³	1.440	1.465	1.404	1.413	1.383	1.565	1.492	1.430	1.430	1.613	1.665	1.560	1.428
<i>μ</i> /cm ⁻¹	7.54	6.75	5.26	4.96	5.53	6.68	5.57	6.11	6.16	37.08	40.23	36.53	5.15
Scan rate/ ^o min ⁻¹	16	8	4	8	12	16	8	8	8	16	8	16	8
No. of reflections (<i>θ</i> < 50 ^o)	7159	7436	6478	8645	5376	6737	7733	6654	6871	6628	6362	6742	8517
No. of data used	3700 (<i>I</i> > 3.0σ(<i>I</i>))	3805 (<i>I</i> > 3.0σ(<i>I</i>))	1421 (<i>I</i> > 2.0σ(<i>I</i>))*	3298 (<i>I</i> > 2.0σ(<i>I</i>))	2310	5172 (<i>I</i> > 2.0σ(<i>I</i>))	4458 (<i>I</i> > 2.0σ(<i>I</i>))	3228 (<i>I</i> > 2.0σ(<i>I</i>))	3189 (<i>I</i> > 2.0σ(<i>I</i>))	4500 (<i>I</i> > 2.0σ(<i>I</i>))	5967 (<i>I</i> > 0.0σ(<i>I</i>))	4121 (<i>I</i> > 2.0σ(<i>I</i>))	5118 (<i>I</i> > 2.5σ(<i>I</i>))
No. of variables	343	361	238	577	472	433	523	469	451	451	433	451	553
<i>R</i> ; <i>R_w</i> ^{<i>a</i>,<i>b</i>}	0.052; 0.054	0.053; 0.072	0.100; 0.107	0.063; 0.075	0.072; 0.075	0.050; 0.069	0.101; 0.156	0.086; 0.142	0.058; 0.072	0.070; 0.121	0.084; 0.083	0.089; 0.144	0.073; 0.092
<i>R1</i> (reflections)							0.066(4458)			0.044(4500)	0.039(4354)	0.053(4121)	
GOF ^{<i>c</i>}	1.25	2.24	1.82	1.22	1.28	1.87	2.30	3.15	1.62	1.98	1.41	1.78	3.21

^{*a*} $R = \sum ||F_o| - |F_c|| / \sum |F_o|$ and $R_w = [\sum w(|F_o| - |F_c|)^2 / \sum w|F_o|^2]^{1/2}$ ($w = 1/\sigma^2(F_o)$). ^{*b*} $R = \sum (F_o^2 - F_c^2) / \sum F_o^2$ and $R_w = [\sum w(F_o^2 - F_c^2)^2 / \sum w(F_o^2)^2]^{1/2}$ ($w = 1/\sigma^2(F_o)$). ^{*c*} $GOF = [\sum w(|F_o| - |F_c|)^2 / (N_o - N_p)]^{1/2}$.

a Rigaku AFC5S refractometer at 27 °C. Intensities were measured by the 2θ - ω scan method using Mo-K α radiation ($\lambda = 0.71069$ Å). Throughout the data collection the intensities of the three standard reflections were measured every 200 reflections as a check of the stability of the crystals and no decay was observed. Intensities were corrected for Lorentz and polarization effects. Absorption corrections were made with ψ scans. Atomic scattering factors were taken from Cromer and Waber the usual tabulation.²⁷ Anomalous dispersion effects were included in F ; the values of $\Delta f'$ and $\Delta f''$ were those of Creagh and McAuley.²⁹ All calculations were performed using the teXsan crystallographic software package.³⁰

Determination of the structures

The structures were solved by Patterson methods (DIRDIF92 PATTY) and refined on F values except for **10b**, **18a** and **18b** refined on F^2 values, since these three complexes were not well-refined on F values. All non-hydrogen atoms were isotropically refined except the rhodium atom refined with anisotropic thermal parameters in **5b**, because of poor crystallinity. The positions of all non-hydrogen atoms except the carbon atoms in **15** were refined with anisotropic thermal parameters by using full-matrix least-squares methods. The refinement for alternative space group for **7** did not yield a good result. The refinements were not well settled in complexes **11a**, **12b** and **19bcf** ($0.1 < \text{shift/error} < 0.2$). All hydrogen atoms were calculated at ideal positions with C–H distances of 0.95 Å).

CCDC reference numbers 169058–169068.

See <http://www.rsc.org/suppdata/dt/b1/b104811m/> for crystallographic data in CIF or other electronic format.

Summary

In this study, reactions of 1-alkynes or electron-deficient-disubstituted alkynes with the P–O chelate complexes [Cp*MCl(MDMPP-*P,O*)] (**1a**: M = Rh; **1b**: M = Ir) and [Cp*MCl(BDMPP-*P,O*)] (**2a**: M = Rh; **2b**: M = Ir), derived from reactions of [Cp*MCl]₂ (M = Rh, Ir) with (2,6-dimethoxyphenyl)diphenylphosphine or bis(2,6-dimethoxyphenyl)phenylphosphine, in the presence of anions led to the formation of unprecedented complexes; (1) a double insertion of 1-alkyne into an Rh–O σ -bond, (2) a single insertion of HC \equiv CCOOR into an Rh–O σ -bond accompanying an extraction of CO from an ester, (3) a single insertion of the disubstituted alkyne into Rh–O or Ir–O σ -bonds, (4) a *cis*-insertion of 1-ethynylbenzene derivatives bearing an electron withdrawing substituent into the P–C bond of the phosphine ligand and a transannular addition between a Rh atom and an *ipso*-carbon atom of the phosphine ligand in rhodium and iridium complexes and (5) formation of a carbene complex and a carbonyl complex by a cleavage of a C–C triple bond with H₂O. The manifold reactivity of alkynes for the P–O chelate complexes was found to depend on alkynes, metals and the P–O chelate ligands. We previously reported that the P–O chelate complexes reacted readily with electron-deficient olefins, leading to a novel insertion of the olefin into the C–H bond adjacent to the M–O bond.¹⁴ These results demonstrated that the P–O chelate complexes were able to lead to unprecedented reactions with alkynes and could play a role as useful starting materials in developing activation of small molecules.

Acknowledgements

The authors would like to thank Professor Shigetoshi Takahashi and Dr Fumie Takei of The Institute of Scientific

and Industrial Research, Osaka University for performing the FAB mass spectrometry measurements. This work was partially supported by a Grant-in Aid for Scientific Research from the Ministry of Education of Japan. We acknowledge the referees who have expended great effort and time and gave useful comments on their reviews.

References

- 1 L. T. Scott, M. J. Cooney and D. Johnels, *J. Am. Chem. Soc.*, 1990, **112**, 4054.
- 2 M. H. Chisholm, *Angew. Chem., Int. Ed. Engl.*, 1991, **30**, 673.
- 3 B. M. Trost, G. Dyker and R. J. Kulawiec, *J. Am. Chem. Soc.*, 1990, **112**, 7809.
- 4 L. S. Liebeskind, R. Chidambaram, D. Mitchell and B. S. Foster, *Pure Appl. Chem.*, 1988, **60**, 27.
- 5 A. G. M. Barrett, J. Mortier, M. Sabat and M. A. Sturgess, *Organometallics*, 1988, **7**, 2553.
- 6 R. Mahe, P. H. Dixneuf and S. Lecolier, *Tetrahedron Lett.*, 1986, **27**, 6333.
- 7 A. G. M. Barrett and N. E. Carpenter, *Organometallics*, 1987, **6**, 2249.
- 8 S. L. Buchwald R. H. Grubbs, *J. Am. Chem. Soc.*, 1983, **105**, 5490.
- 9 M. I. Bruce, *Chem. Rev.*, 1991, **91**, 197 and refs. therein.
- 10 Y. Yamamoto, R. Sato, F. Matsuo, C. Sudoh and T. Igoshi, *Inorg. Chem.*, 1996, **35**, 2329.
- 11 Y. Yamamoto, R. Sato, M. Ohshima, F. Matsuo and C. Sudoh, *J. Organomet. Chem.*, 1995, **489**, C68.
- 12 X.-H. Han and Y. Yamamoto, *J. Organomet. Chem.*, 1998, **561**, 157.
- 13 Y. Yamamoto, K. Kawasaki and S. Nishimura, *J. Organomet. Chem.*, 1999, **587**, 49.
- 14 Y. Yamamoto, X.-H. Han, K. Sugawara and S. Nishimura, *Angew. Chem.*, 1999, **112**, 1318; Y. Yamamoto, X.-H. Han, K. Sugawara and S. Nishimura, *Angew. Chem., Int. Ed.*, 1999, **38**, 1242; Y. Yamamoto, X.-H. Han, S. Nishimura, K. Sugawara, N. Nezu and T. Tanase, *Organometallics*, 2001, **20**, 266.
- 15 Y. Yamamoto, T. Tanase, C. Sudoh and T. Turuta, *J. Organomet. Chem.*, 1998, **569**, 29.
- 16 H. E. Bryndza, J. C. Calabrese and S. S. Wreford, *Organometallics*, 1984, **3**, 1603.
- 17 The insertion of alkynes into the Pt–OH bond has cited: H. Jin, PhD Thesis, The Australian National University, 1990; in ref. 18, but details were not reported.
- 18 M. A. Bennett, H. Jin, S. Li, L. M. Rendina and A. C. Willis, *J. Am. Chem. Soc.*, 1995, **117**, 8335.
- 19 Y. Yamamoto, X.-H. Han and J.-F. Ma, *Angew. Chem., Int. Ed.*, 2000, **39**, 1965.
- 20 Y. Yamamoto and K. Sugawara, *J. Chem. Soc., Dalton Trans.*, 2000, 2896.
- 21 J. A. Cabeza, I. Rio, R. J. Franco, F. Grepioni and V. Riera, *Organometallics*, 1997, **16**, 2763.
- 22 T. Yamamoto, J. Ishizu, T. Kohara, S. Komiya and A. Yamamoto, *J. Am. Chem. Soc.*, 1980, **102**, 3758.
- 23 T. Yamamoto, S. Miyashita, Y. Naito, S. Komiya, T. Ito and A. Yamamoto, *Organometallics*, 1982, **1**, 808.
- 24 Complex **14** was formed by an addition of H₂O to an initially generated vinylidene complex and the subsequent cleavage of a C–C bond. Details of this reaction will be reported elsewhere.
- 25 H. M. Walborsky and G. E. Niznik, *J. Org. Chem.*, 1972, **37**, 187.
- 26 M. Wada, A. Higashimura and A. Tsuboi, *J. Chem. Res. (S)*, 1985, 38; M. Wada, A. Higashimura and A. Tsuboi, *J. Chem. Res. (M)*, 1985, 467.
- 27 D. T. Cromer and J. T. Waber, *International Tables for X-Ray Crystallography*, Kynoch Press, Birmingham, England, 1974, vol. 4, Table 2.2A.
- 28 J. A. Ibers and W. C. Hamilton, *Acta Crystallogr.*, 1964, **17**, 781.
- 29 D. C. Creagh and W. McAuley, *International Tables for Crystallography*, Kluwer, Boston, MA, 1992, vol. C, Table 4.2.6.8 pp. 219–222.
- 30 TEXSANX: Crystal Structure Analysis Package, Molecular Structure Corporation Houston, TX, 1985 and 1992.